CP&L
A Progress Energy Company

John S. Keenan
Vice President
Brunswick Nuclear Plant

10 CFR 50.90

NOV 2 2 2002

SERIAL: BSEP 02-0186
TSC-2002-03

U. S. Nuclear Regulatory Commission
ATTN: Document Control Desk
Washington, DC 20555-0001

SUBJECT: Brunswick Steam Electric Plant, Unit Nos. 1 and 2
Docket Nos. 50-325 and 50-324/License Nos. DPR-71 and DPR-62
Response to Request for Additional Information, Proposed License Amendment to Revise Pressure-Temperature Curve Limits
(NRC TAC Nos. MB5579 and MB5580)

Ladies and Gentlemen:

On June 26, 2002 (i.e., Serial: BSEP 02-0121), Carolina Power & Light (CP&L) Company requested a revision to the Technical Specifications for the Brunswick Steam Electric Plant (BSEP), Units 1 and 2. The proposed license amendments revise the reactor coolant system pressure-temperature (P-T) limits curves for operation to 32 effective full power years.

On August 23, 2002, the NRC requested additional information regarding the Westinghouse reactor vessel fluence analysis used to support the proposed P-T limits curves. The information enclosed provides an analysis of the pool critical assembly (PCA) activity dosimetry benchmark experiment, an analysis of the H. B. Robinson dosimetry, and analysis of the available surveillance capsule and ex-vessel dosimetry for BSEP.

Please refer any questions regarding this submittal to Mr. Edward T. O'Neil, Manager - Support Services, at (910) 457-3512.

Sincerely,

John S. Keenan

John S. Keenan

WRM/wrm

Enclosure: Report LTR-REA-02-126, "Neutron Exposure Evaluations for the Core Shroud and Pressure Vessel Brunswick Units 1 and 2"

P.O. Box 10429
Southport, NC 28461

T > 910.457.2496
F > 910.457.2803

A001

John S. Keenan, having been first duly sworn, did depose and say that the information contained herein is true and correct to the best of his information, knowledge and belief; and the sources of his information are officers, employees, and agents of Carolina Power & Light Company.

Dean L. Mash
Notary (Seal)

My commission expires: August 29, 2004

cc (with enclosure):

U. S. Nuclear Regulatory Commission, Region II
ATTN: Mr. Luis A. Reyes, Regional Administrator
Sam Nunn Atlanta Federal Center
61 Forsyth Street, SW, Suite 23T85
Atlanta, GA 30303-8931

U. S. Nuclear Regulatory Commission
ATTN: Mr. Theodore A. Easlick, NRC Senior Resident Inspector
8470 River Road
Southport, NC 28461-8869

U. S. Nuclear Regulatory Commission **(Electronic Copy Only)**
ATTN: Ms. Brenda L. Mozafari (Mail Stop OWFN 8G9)
11555 Rockville Pike
Rockville, MD 20852-2738

U. S. Nuclear Regulatory Commission **(Electronic Copy Only)**
ATTN: Mr. Leonard Olshan (Mail Stop OWFN 8G9)
11555 Rockville Pike
Rockville, MD 20852-2738

Ms. Jo A. Sanford
Chair - North Carolina Utilities Commission
P.O. Box 29510
Raleigh, NC 27626-0510

Ms. Beverly O. Hall, Section Chief
Radiation Protection Section, Division of Radiation Protection
North Carolina Department of Environment and Natural Resources
3825 Barrett Drive
Raleigh, NC 27609-7221

LTR-REA-02-126

Neutron Exposure Evaluations for the Core Shroud and Pressure Vessel Brunswick Units 1 and 2

S. L. Anderson
Radiation Engineering and Analysis

November 2002

Benchmarking Information to Support Brunswick Units 1 and 2 Fluence Analysis

1.0 Background

The purpose of this writeup is to provide supplemental information to demonstrate that the methodology used in the fluence analysis for Brunswick Units 1 and 2 meets the requirements of Regulatory Guide 1.190, "Calculational and Dosimetry Methods for Determining Pressure Vessel Neutron Fluence".[1]

In performing the fast neutron exposure evaluations for the Brunswick Units 1 and 2 reactors, plant specific forward transport calculations were carried out using the three-dimensional flux synthesis technique described in Section 1.3.4 of Regulatory Guide 1.190.[1] In these analyses, the following single channel synthesis equation was employed:

$$\varphi(r,\theta,z) = \varphi(r,\theta) * \frac{\varphi(r,z)}{\varphi(r)}$$

where $\phi(r,\theta,z)$ is the synthesized three-dimensional neutron flux distribution, $\phi(r,\theta)$ is the transport solution in r,θ geometry, $\phi(r,z)$ is the two-dimensional solution for a cylindrical reactor model using the actual axial core power distribution, and $\phi(r)$ is the one-dimensional solution for a cylindrical reactor model using the same source per unit height as that used in the r,θ two-dimensional calculation.

All of the transport calculations supporting the Brunswick Units 1 and 2 evaluations were carried out using the DORT two-dimensional discrete ordinates code version 3.1[2] and the BUGLE-96 cross–section library.[3] The BUGLE-96 library, derived from the ENDF/B-VI data files, provides a 67 group coupled neutron-gamma ray cross-section data set produced specifically for light water reactor application. In these analyses, anisotropic scattering was treated with a P_3 legendre expansion and the angular discretization was modeled with an S_8 order of angular quadrature.

The methodology qualification described in Regulatory Guide 1.190 requires comparisons of calculated foil reaction rates with measurements obtained from benchmark and operating reactor irradiations. In performing the required calculation to measurement comparisons, the results of the neutron transport calculations are combined with dosimetry reaction cross-sections to produce the calculated reaction rates for each of the sensors included in the various measurement programs. For the Brunswick application, the dosimetry cross-sections were taken from the SNLRML dosimetry cross-section library.[4] The cross-sections extracted from the SNLRML library for use in the benchmarking comparisons were derived from the ENDF/B-VI evaluations.

The methodology qualification described in Regulatory Guide 1.190 requires an analytical uncertainty analysis (Section 1.4.1), comparisons with benchmark measurements (Section 1.4.2), and comparisons with operating reactor measurements (Section 1.4.2.1).

2.0 Dosimetry Cross-Section Comparisons

Since the dosimetry cross-sections processed from the SNLRML library are a key input to the calculation to measurement comparisons that are required in order to benchmark the calculational methodology, the individual sensor reaction cross-sections were evaluated against the results of benchmark field irradiations performed at the National Institute for Standards and Technology (NIST). The results of those evaluations are provided in this section.

In ASTM E 261-98, "Standard Practice for Determining Neutron Fluence Rate, Fluence, and Spectra by Radioactivation Techniques", fission spectrum averaged cross-sections applicable to the ^{235}U thermal fission field are provided for threshold activation detectors that are typically used in power and research reactor irradiations. In this data compilation, both calculated and measured spectrum averaged cross-sections are given along with their uncertainties. The data provided in Tables 2-1 and 2-2 have been extracted from Table 3 of ASTM E 261-98 as representative of the foil sets typically used in power reactor irradiations as well as of those used in the Pool Critical Assembly (PCA) benchmark irradiations.

As a test of the dosimetry cross-sections used in the methodology benchmarking studies, data from the SNLRML library were processed using the multi-group ^{235}U fission spectrum supplied with the BUGLE-96 library. Results of that cross-section processing are provided in Tables 2-3 and 2-4 for the power reactor and PCA sensor sets, respectively.

The comparisons shown in Tables 2-3 and 2-4 are in excellent agreement with those from ASTM Standard E261 (Tables 2-1 and 2-2) thereby demonstrating that the processed SNLRML dosimetry cross-sections are appropriate for use in the methodology benchmarking studies that require comparisons of calculated and measured reaction rates in both test reactor and power reactor environments.

From Table 2-1, it is also noted that $^{46}Ti(n,p)^{46}Sc$ is the only reaction for which the observed C/M ratio (0.899) differs from unity by more than one standard deviation (6.86%). Furthermore, the C/M ratio of 0.899 implies that calculated reaction rates for this reaction would tend to be low relative to measurement due solely to the dosimetry cross-section. Therefore, in the comparisons noted in subsequent sections of this writeup, the $^{46}Ti(n,p)^{46}Sc$ reaction has been excluded from the evaluations.

Table 2-1

^{235}U Fission Spectrum Averaged Cross-Sections for Power Reactor Sensor Sets

Reaction	Calculation (mb)[1]	Measured (mb)[2]	C/M[3]
^{63}Cu(n,α)^{60}Co	0.521 (2.85%,6.05%)	0.50 (11%)	1.042 (12.87%)
^{46}Ti(n,p)^{46}Sc	10.43 (2.46%,5.40%)	11.6 (3.45%)	0.899 (6.86%)
^{54}Fe(n,p)^{54}Mn	80.18 (2.17%,4.69%)	80.5 (2.86%)	0.996 (5.91%)
^{58}NI(n,p)^{58}Co	105.69 (2.43%,4.52%)	108.5 (5.0%)	0.974 (7.16%)
^{238}U(n,f)FP	306.23 (0.53%,4.21%)	309.0 (2.6%)	0.991 (4.98%)
^{237}Np(n,f)FP	1330.1 (9.33%,4.31%)	1344.0 (4.0%)	0.990 (4.98%)

Table 2-2

^{235}U Fission Spectrum Averaged Cross-Sections for PCA Sensor Sets

Reaction	Calculation (mb)[1]	Measured (mb)[2]	C/M[3]
^{27}Al(n,α)^{24}Na	0.727 (1.40%,6.95%)	0.706 (3.97%)	1.030 (8.13%)
^{58}NI(n,p)^{58}Co	105.69 (2.43%,4.52%)	108.5 (5.0%)	0.974 (7.16%)
^{115}In(n,n')^{115m}In	186.35 (2.17%,4.17%)	190.3 (3.84%)	0.979 (6.07%)
^{103}Rh(n,n')^{103m}Rh	706.02 (3.1%,4.14%)	733.0 (5.2%)	0.963 (7.33%)
^{238}U(n,f)FP	306.23 (0.53%,4.21%)	309.0 (2.6%)	0.991 (4.98%)
^{237}Np(n,f)FP	1330.1 (9.33%,4.31%)	1344.0 (4.0%)	0.990 (4.98%)

Notes:

1. The cross-section and spectrum components of uncertainty, respectively, are in parentheses.
2. The measurement uncertainty appears in parentheses.
3. The uncertainty represents a sum in quadrature of the measurement and calculational uncertainty.

Table 2-3

^{235}U Fission Spectrum Averaged Cross-Sections for Power Reactor Sensor Sets

Reaction	Calculation (mb)	Measured (mb)	C/M
$^{63}Cu(n,\alpha)^{60}Co$	0.523	0.50	1.046
$^{46}Ti(n,p)^{46}Sc$	10.3	11.6	0.888
$^{54}Fe(n,p)^{54}Mn$	80.3	80.5	0.998
$^{58}Ni(n,p)^{58}Co$	106	108.5	0.977
$^{238}U(n,f)FP$	306	309.0	0.991
$^{237}Np(n,f)FP$	1330	1344.0	0.990

Table 2-4

^{235}U Fission Spectrum Averaged Cross-Sections for PCA Sensor Sets

Reaction	Calculation (mb)	Measured (mb)	C/M
$^{27}Al(n,\alpha)^{24}Na$	0.729	0.706	1.033
$^{58}Ni(n,p)^{58}Co$	106	108.5	0.977
$^{115}In(n,n')^{115m}In$	186	190.3	0.977
$^{103}Rh(n,n')^{103m}Rh$	706	733.0	0.963
$^{238}U(n,f)FP$	306	309.0	0.990
$^{237}Np(n,f)FP$	1330	1344.0	0.990

3.0 PCA Benchmark Comparisons

The pressure vessel simulator comparisons used in the qualification of the transport methodology are based on an analysis of the PCA 12/13 configuration (see References 5, 6, and 7). A schematic description of this configuration is provided in Figures 3-1 and 3-2. A plan view of the PCA reactor and pressure vessel simulator showing materials characteristic of the core axial midplane is shown in Figure 3-1, whereas, a section view through the center of the mockup is shown in Figure 3-2. The configuration described in Figures 3-1 and 3-2 was developed from dimensional information provided in Reference 6 and reflects the latest available geometric data for the simulator.

During the PCA experiments, measurements were taken at several locations within the mockup to provide traverse data extending from the reactor core outward through the pressure vessel simulator and on into the void box. The specific measurement locations are illustrated on Figure 3-1 and listed in Table 3-1. From Figure 3-1, it may be noted that all of the measurements of interest were obtained on the lateral centerline of the mockup. Furthermore, all of the measurement points were also positioned on the axial midplane of the simulator.

The measurement locations specified in Table 3-1 provide data sufficient to generate calculation/measurement comparisons throughout the entire 12/13 configuration. Data from locations A4, A5, and A6 establish the means for verification of calculated exposure gradients within the pressure vessel wall itself. Since measurements at operating power reactors can, at best, provide data in the downcomer region internal to the pressure vessel or in the reactor cavity external to the vessel wall, these PCA data points located interior to the thick walled vessel establish a key set of comparisons to aid in the accurate determination of exposure gradients within the pressure vessel wall.

Table 3-1

Summary of Measurement Locations Within the PCA 12/13 Configuration

Location	ID	Y(cm)
Core Center	A0	-20.57
Thermal Shield Front	A1	12.0
Thermal Shield Back	A2	23.8
Pressure Vessel Front	A3	29.7
Pressure Vessel 1/4T	A4	39.5
Pressure Vessel 1/2T	A5	44.7
Pressure Vessel 3/4T	A6	50.1
Void Box	A7	59.1

Figure 3-1

PCA 12/13 Configuration - X,Y Geometry

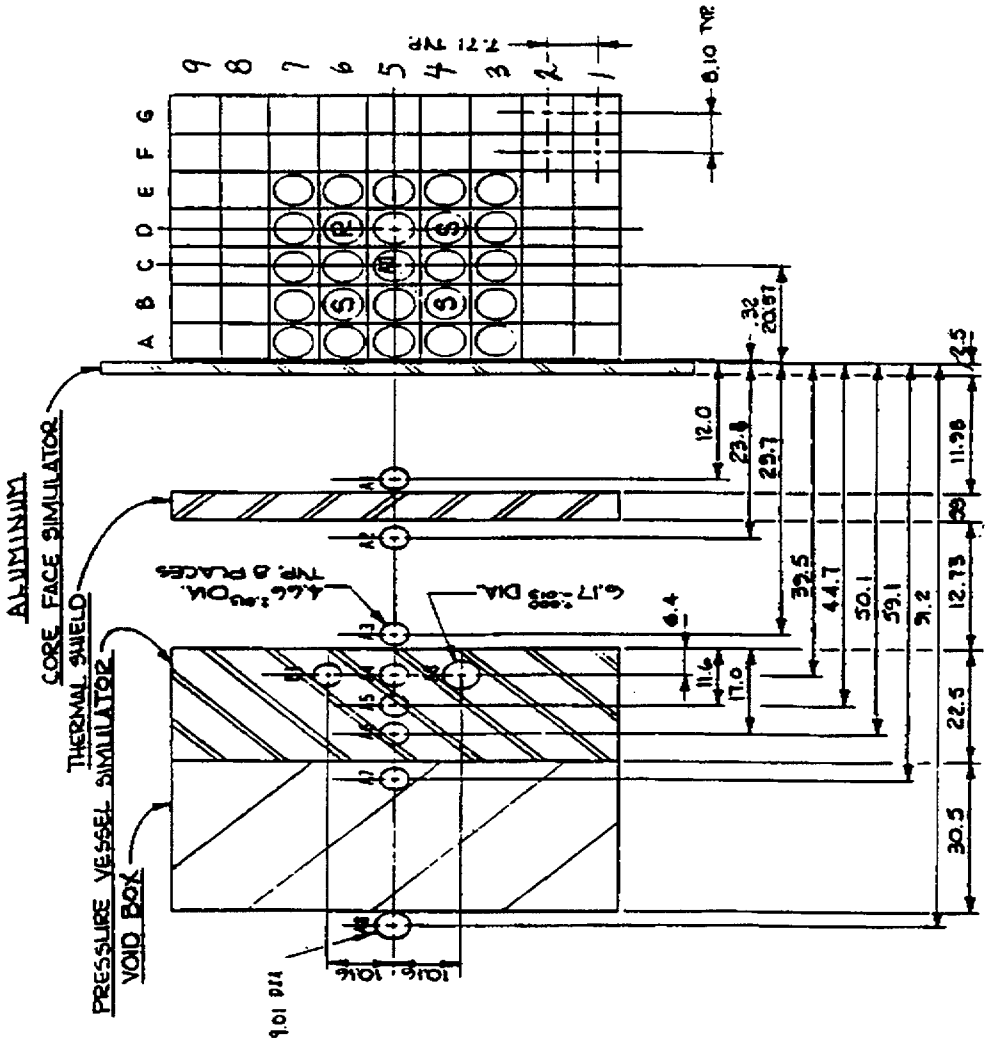

Figure 3-2

PCA 12/13 Configuration - Y,Z Geometry

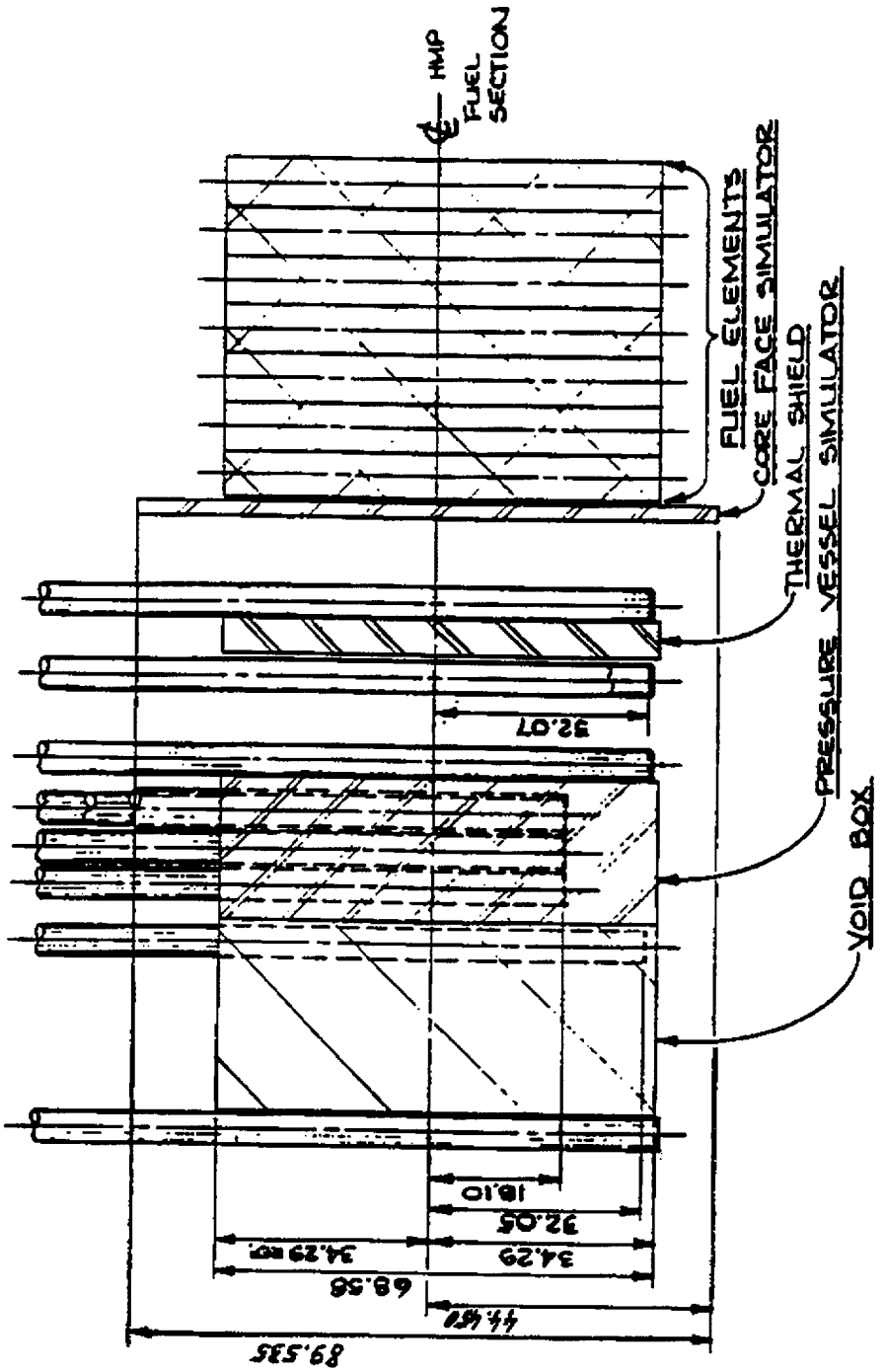

3.1 Two-Dimensional Analysis

The initial neutron transport analysis of the PCA 12/13 configuration was carried out using the conventional three-dimensional synthesis technique. That is, the evaluation consisted of two DORT two-dimensional discrete ordinates transport calculations, one in x,y geometry and one in y,z geometry, as well as a single one-dimensional DORT calculation in planar (y) geometry, that were combined to synthesize a three-dimensional solution throughout the PCA simulator. The synthesis was carried out using the following relationship:

$$\phi_g(x,y,z) = \phi_g(x,y) * \frac{\phi_g(y,z)}{\phi_g(y)}$$

where: $\phi_g(x,y,z)$ = The group-g neutron flux at position x,y,z within the simulator geometry.
$\phi_g(x,y)$ = The group-g neutron flux solution from the x,y DORT computation.
$\phi_g(y,z)$ = The group-g neutron flux solution from the y,z DORT computation.
$\phi_g(y)$ = The group-g neutron flux solution from the y DORT computation.

In this synthesis approach the ratio $[\phi_g(y,z)]/[\phi_g(y)]$ represents the energy and spatially dependent axial shape factor that accounts for the finite height of the PCA core as well as for the axial leakage effects introduced by the simulator geometry.

In the calculation of the PCA 12/13 configuration, all of the DORT computations were carried out in 67 energy groups (47 neutron, 20 gamma-ray) using a P_3 cross-section expansion and an S_8 order of angular quadrature. The analyses were carried out using the BUGLE-96 cross-section library. The geometric models used in the calculations consisted of 71 x 131, 131 x 71, and 131 spatial mesh cell arrays for the x,y, y,z, and y calculations, respectively. Material descriptions for each of the regions comprising the simulator geometry were taken as specified in References 5, 6, and 7. Likewise, the spatial distribution of the neutron source within the PCA core was obtained directly from References 5 through 7. In generating the energy dependent source for use in the transport calculations, the specified spatial distribution was coupled with the ENDF/B-VI ^{235}U fission spectrum supplied with the BUGLE-96 library. Sensor reaction rates for direct comparison with the published PCA measurements were obtained by folding the synthesized three-dimensional neutron flux distribution using dosimeter reaction cross-sections from the SNLRML library.

Measured data from the PCA experiments using the 12/13 simulator configuration have been documented and discussed extensively in References 5, 6, and 7. In these documents, individual sensor measurements were provided in terms of either equivalent fission flux per source neutron or absolute reaction rates per source neutron. Measured data were supplied for a variety of reactions with responses spanning the fast neutron energy range. For the comparisons presented in this report, all equivalent fission fluxes were converted to absolute reaction rates using fission spectrum averaged reaction cross-sections that were also reported in the PCA documentation. In particular, the following reaction cross-sections were employed to perform the required conversions:

Reaction	σ_f (barns/atom)
$^{27}Al(n,\alpha)^{24}Na$	0.000705
$^{58}Ni(n,p)^{58}Co$	0.1085
$^{115}In(n,n')^{115m}In$	0.189
$^{103}Rh(n,n')^{103m}Rh$	0.733
$^{238}U(n,f)FP$	0.308
$^{237}Np(n,f)FP$	1.334

The appropriate measured reaction rates used for comparison with analytical prediction are summarized in Table 3-2.

In regard to the measured reaction rates listed in Table 3-2 it is important to note that, based on discussions contained in Reference 7, the ^{238}U and ^{237}Np data for locations within the pressure vessel wall (A4, A5, and A6) differ somewhat from the reaction rates given in References 5 and 6. In Reference 6, a 10% bias was noted between fission chamber measurements and solid state track recorder (SSTR) data. As a result, recommended reaction rates were taken to be the average of the two data sets. This recommendation was propagated into Reference 5. In Reference 7, however, it is noted that the observed bias was determined to be caused by perturbations in the neutron field introduced by the presence of the fission chamber structure. Therefore, the SSTR measurements provided a more accurate representation of the $^{238}U(n,f)$ and $^{237}Np(n,f)$ reaction rates within the pressure vessel wall. The data listed in Table 3-2 incorporate only the SSTR results for positions A4, A5, and A6. Fission rate data for all other locations within the 12/13 configuration remain as reported in References 5 and 6.

Results of the DORT analysis of the PCA 12/13 configuration using the two-dimensional synthesis approach are provided in Tables 3-3 and 3-4. In Table 3-3, the calculated sensor reaction rates at each of the measurement locations are provided. In Table 3-4, the corresponding ratios of measured to calculated reaction rates, [M]/[C], are given. An examination of Table 3-4 shows excellent agreement between calculation and measurement near the front face of the simulator. However, a trend toward underprediction at increased depth within the pressure vessel wall as well as within the void box external to the pressure vessel is also observed with M/C ratios exceeding 20% in the void box region located behind the simulator.

3.2 Three Dimensional Analysis

In an attempt to determine if the observed trend towards underprediction with increased depth in the pressure vessel simulator is due to inadequacies in transport cross-sections or in the application of the two-dimensional synthesis technique to the analysis of a small reactor system, the PCA analysis was repeated using the TORT three-dimensional discrete ordinates transport code[2] in x,y,z geometry. The TORT analysis was also performed using the BUGLE-96 cross-section library with a P_3 scattering cross-section expansion and an S_8 order of angular quadrature. The geometric model constructed for the TORT application consisted of 15, 39, and 39 spatial mesh intervals in the x, y, and z directions, respectively.

The results of the TORT three-dimensional calculations are provided in Tables 3-5 and 3-6. In Table 3-5, the calculated sensor reaction rates at the PCA measurement

locations are given. In Table 3-6, the M/C ratios observed with the BUGLE-96 analyses are provided.

An examination of Table 3-6 shows a remarkable improvement with the three-dimensional analysis. Based on the average foil M/C ratios, the BUGLE-96 calculation falls within $\pm$ 3% of the measured values at all measurement locations. Of the 36 individual foil reaction rate M/C ratios only one (the ^{238}U(n,f) reaction at location A3) differs from unity by more than 5%. Treating the entire 36 sample set as a data base yields an average M/C ratio of 1.00 with an associated standard deviation of 3%.

These comparisons demonstrate that the ENDF/B-VI neutron transport cross-section sets provided in the BUGLE-96 library provide an essentially unbiased solution throughout the full thickness of the pressure vessel simulator. Furthermore, the improvement in the solution with the full three-dimensional approach indicates that the trend towards underprediction with depth into the pressure vessel that was observed in the initial synthesis based analysis was not caused by the BUGLE-96 cross-section data. Rather, this trend towards underprediction was caused by the application of the synthesis approach to a relatively small reactor system, an issue that is mitigated when the methodology is applied to the much larger power reactor designs.

Table 3-2

Measured Reaction Rates Applicable to the PCA 12/13 Configuration

	Reaction Rate [rps/source neutron]					
Location	**^{27}Al(n,α)**	**^{58}Ni(n,p)**	**^{115}In(n,n')**	**^{103}Rh(n,n')**	**^{238}U(n,f)**	**^{237}Np(n,f)**
A1	5.48e-33	6.31e-31	1.05e-30	4.06e-30		
A2	7.16e-34	6.72e-32	1.14e-31	4.50e-31		
A3	3.13e-34	2.50e-32	3.68e-32	1.47e-31	5.91e-32	3.05e-31
A4	7.15e-35	5.69e-33	1.11e-32	5.67e-32	1.79e-32	1.20e-31
A5	2.92e-35	2.25e-33	5.20e-33	3.24e-32	7.88e-33	6.56e-32
A6	1.12e-35	7.99e-34	2.23e-33	1.67e-32	3.26e-33	3.47e-32
A7			6.43e-34	4.83e-33	8.65e-34	9.60e-33

Table 3-3

Calculated Reaction Rates Applicable to the PCA 12/13 Configuration
DORT Synthesis Approach

	Reaction Rate [rps/source neutron]					
Location	**^{27}Al(n,α)**	**^{58}Ni(n,p)**	**^{115}In(n,n')**	**^{103}Rh(n,n')**	**^{238}U(n,f)**	**^{237}Np(n,f)**
A1	5.39e-33	5.97e-31	9.97e-31	3.94e-30		
A2	7.00e-34	6.40e-32	1.08e-31	4.48e-31		
A3	3.18e-34	2.44e-32	3.67e-32	1.45e-31	6.21e-32	2.75e-31
A4	7.07e-35	5.43e-33	1.10e-32	5.53e-32	1.70e-32	1.14e-31
A5	2.83e-35	2.13e-33	5.00e-33	2.96e-32	7.33e-33	6.26e-32
A6	1.07e-35	7.85e-34	2.13e-33	1.47e-32	2.93e-33	3.16e-32
A7			5.13e-34	3.61e-33	7.03e-34	7.83e-33

Table 3-4

Reaction Rate M/C Comparisons Applicable to the PCA 12/13 Configuration
DORT Synthesis Approach

	Reaction						
Location	**^{27}Al(n,α)**	**^{58}Ni(n,p)**	**^{115}In(n,n')**	**^{103}Rh(n,n')**	**^{238}U(n,f)**	**^{237}Np(n,f)**	**Average**
A1	1.02	1.06	1.05	1.03			1.04
A2	1.02	1.05	1.05	1.00			1.03
A3	0.99	1.03	1.00	1.02	0.95	1.11	1.02
A4	1.01	1.05	1.01	1.03	1.05	1.05	1.03
A5	1.03	1.06	1.04	1.09	1.08	1.05	1.06
A6	1.05	1.02	1.05	1.14	1.11	1.10	1.08
A7			1.25	1.34	1.23	1.23	1.26

Table 3-5

Calculated Reaction Rates Applicable to the PCA 12/13 Configuration
TORT Three-Dimensional Approach

	Reaction Rate [rps/source neutron]					
Location	$^{27}Al(n,\alpha)$	$^{58}Ni(n,p)$	$^{115}In(n,n')$	$^{103}Rh(n,n')$	$^{238}U(n,f)$	$^{237}Np(n,f)$
A1	5.49e-33	6.07e-31	1.01e-30	4.00e-30		
A2	7.14e-34	6.57e-32	1.12e-31	4.64e-31		
A3	3.28e-34	2.53e-32	3.84e-32	1.52e-31	6.47e-32	2.90e-31
A4	7.46e-35	5.70e-33	1.15e-32	5.89e-32	1.79e-32	1.21e-31
A5	3.01e-35	2.24e-33	5.27e-33	3.17e-32	7.70e-33	6.71e-32
A6	1.15e-35	8.29e-34	2.26e-33	1.60e-32	3.09e-33	3.43e-32
A7			6.20e-34	4.60e-33	8.33e-34	9.97e-33

Table 3-6

Reaction Rate M/C Comparisons Applicable to the PCA 12/13 Configuration
BUGLE-96 TORT Three-Dimensional Approach

	Reaction Rate [rps/source neutron]						
Location	$^{27}Al(n,\alpha)$	$^{58}Ni(n,p)$	$^{115}In(n,n')$	$^{103}Rh(n,n')$	$^{238}U(n,f)$	$^{237}Np(n,f)$	Average
A1	1.00	1.04	1.04	1.01			1.02
A2	1.00	1.02	1.02	0.97			1.00
A3	0.95	0.99	0.96	0.97	0.91	1.05	0.97
A4	0.96	1.00	0.96	0.96	1.00	0.99	0.98
A5	0.97	1.01	0.99	1.02	1.02	0.98	1.00
A6	0.98	0.96	0.99	1.05	1.05	1.01	1.01
A7			1.04	1.05	1.04	0.96	1.02

$$\phi_g(r,\theta,z) = \phi_g(r,\theta) * \frac{\phi_g(r,z)}{\phi_g(r)}$$

where: $\phi_g(r,\theta,z)$ = The group-g neutron flux at position r,θ,z within the reactor geometry.
$\phi_g(r,\theta)$ = The group-g neutron flux solution from the r,θ DORT computation.
$\phi_g(r,z)$ = The group-g neutron flux solution from the r,z DORT computation.
$\phi_g(r)$ = The group-g neutron flux solution from the r DORT computation.

In this synthesis approach the ratio $[\phi_g(r,z)]/[\phi_g(r)]$ represents the energy and spatially dependent axial shape factor that accounts for the finite height of the reactor core as well as for the axial leakage effects introduced by the H. B. Robinson geometry.

In the calculation of the H. B. Robinson configuration, all of the DORT computations were carried out in 67 energy groups (47 neutron, 20 gamma-ray) using a P_3 cross-section expansion and an S_8 order of angular quadrature. Analyses were carried out using the BUGLE-96 cross-section library. The geometric models used in the calculations consisted of 155 x 97, 137 x 223, and 137 spatial mesh cell arrays for the r,θ, r,z, and r calculations, respectively. Material descriptions for each of the regions comprising the simulator geometry were taken as specified in References 8 and 9. Likewise, the spatial distribution of the neutron source within the H. B. Robinson core was obtained directly from Reference 8. In generating the energy dependent source for use in the transport calculations, the specified spatial distribution was coupled with the ENDF/B-VI uranium and plutonium isotopic fission spectra supplied with the BUGLE-96 library. Calculated sensor reaction rates for direct comparison with the published H. B. Robinson measurements were obtained by folding the synthesized three-dimensional neutron flux distribution with the appropriate dosimeter reaction cross-sections from the SNLRML library.

Results of the DORT analysis of the H. B. Robinson configuration are provided in Tables 4-1 through 4-3 and in Figures 4-1 through 4-4. In Tables 4-1 and 4-2, the calculated and measured sensor reaction rates at the 20 degree in-vessel surveillance capsule and the 0 degree midplane ex-vessel cavity sensor set location are provided. Also given in Tables 4-1 and 4-2 are the corresponding ratios of measured to calculated reaction rates, (M/C), for each sensor reaction.

An examination of Tables 4-1 and 4-2 and Figures 4-1 through 4-4 shows excellent agreement between calculation and measurement. Based on the average foil M/C ratios, the BUGLE-96 calculation falls within 2% of the measured values at both the in-vessel and ex-vessel locations. The average M/C value of 1.02 observed both in- and ex-vessel is in excellent agreement with the results obtained from the PCA evaluations performed with TORT. These comparisons further demonstrate that the ENDF/B-VI neutron transport cross-sections provided in the BUGLE-96 library are acceptable for LWR fluence calculations out through the reactor cavity external to the pressure vessel.

The gradient data comparisons provided in Figures 4-1 through 4-4, further demonstrate that the synthesis approach produces acceptable results over the entire height of the reactor core. In addition, the comparison data given in Table 4-3 show good consistency

among the four sets of gradient data and the in-vessel and ex-vessel multiple foil sensor sets.

Table 4-1

Reaction Rate M/C Comparisons for the H. B. Robinson Benchmark
20 Degree In- Vessel Measurement Location

	Calculated	Measured	M/C
$^{63}Cu(n,\alpha)^{60}Co$	3.85e-17	3.98e-17	1.03
$^{54}Fe(n,p)^{54}Mn$	3.79e-16	3.83e-15	1.01
$^{58}Ni(n,p)^{58}Co$	5.13e-15	4.88e-15	0.95
$^{238}U(n,f)FP$	1.68e-14	1.80e-14	1.07
$^{237}Np(n,f)FP$	1.18e-13	1.20e-13	1.02
Average			1.02
% Standard Deviation			4

Table 4-2

Reaction Rate M/C Comparisons for the H. B. Robinson Benchmark
0 Degree Ex- Vessel Measurement Location

	Calculated	Measured	M/C
$^{63}Cu(n,\alpha)^{60}Co$	3.88e-19	4.01e-19	1.03
$^{54}Fe(n,p)^{54}Mn$	3.53e-17	3.59e-17	1.02
$^{58}Ni(n,p)^{58}Co$	5.32e-17	5.29e-17	0.99
$^{238}U(n,f)FP$	2.44e-16	2.72e-16	1.01
Average			1.02
% Standard Deviation			2

Table 4-3

Summary of Multiple Foil and Gradient Chain M/C Ratios

Data Set	Number Of Samples	Average M/C	Std. Dev. (%)
20 Deg. In-Vessel Multiple Foil Set	5	1.02	4
0 Deg. Ex-Vessel Multiple Foil Set	4	1.02	2
0 Deg. Ex-Vessel Iron Gradient	15	1.04	7
12 Deg. Ex-Vessel Iron Gradient	14	0.95	11
30 Deg. Ex-Vessel Iron Gradient	15	1.03	12
45 Deg. Ex-Vessel Iron Gradient	12	1.09	8

Figure 4-1

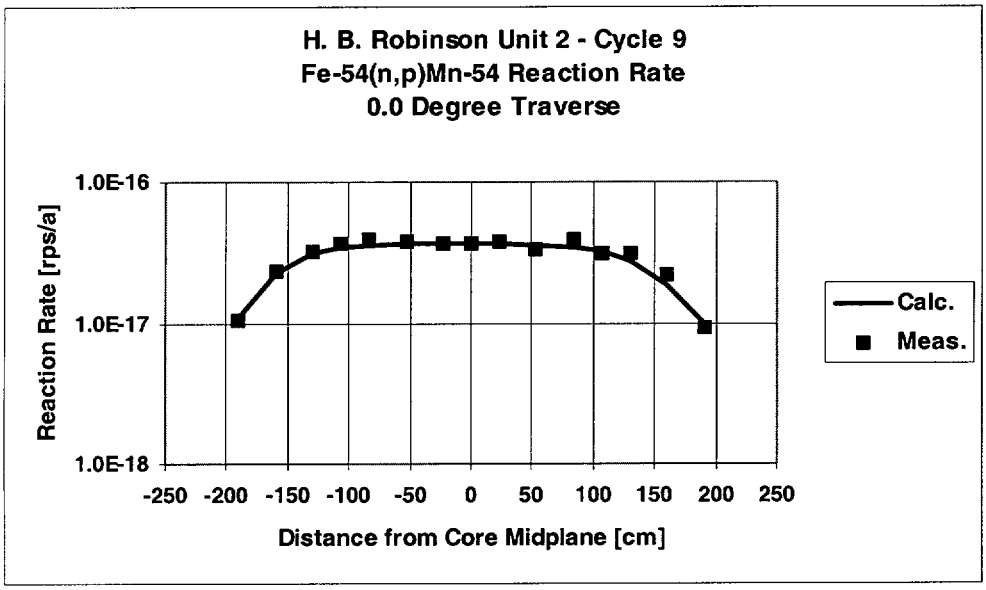

Range of M/C Values 0.94 - 1.09
Average M/C = 1.04
Standard Deviation = 7%

Figure 4-2

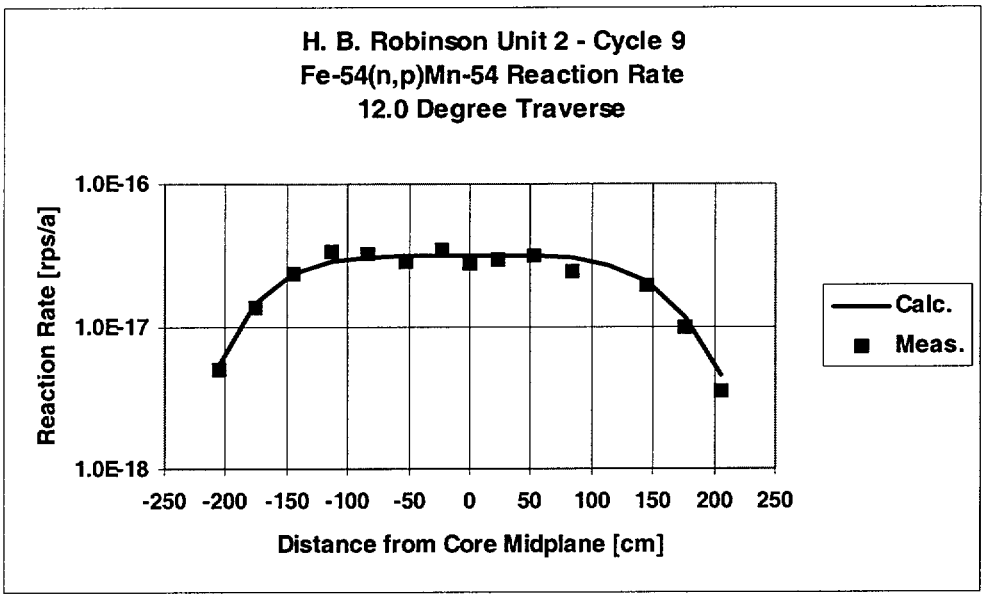

Range of M/C Values 0.79 - 1.18
Average M/C = 0.95
Standard Deviation = 11%

Figure 4-3

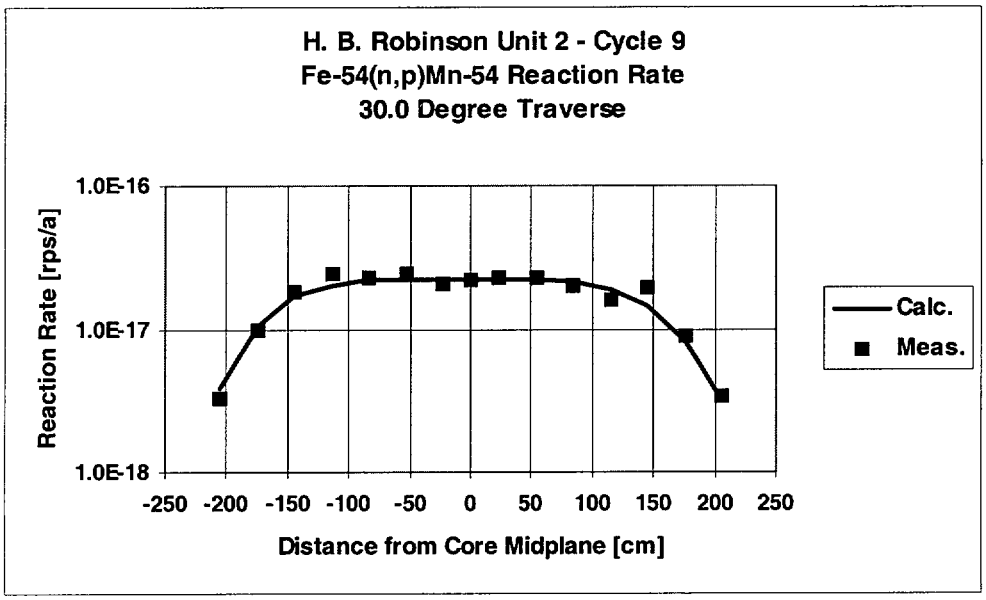

Range of M/C Values 0.84 - 1.33
Average M/C = 1.03
Standard Deviation = 12%

Figure 4-4

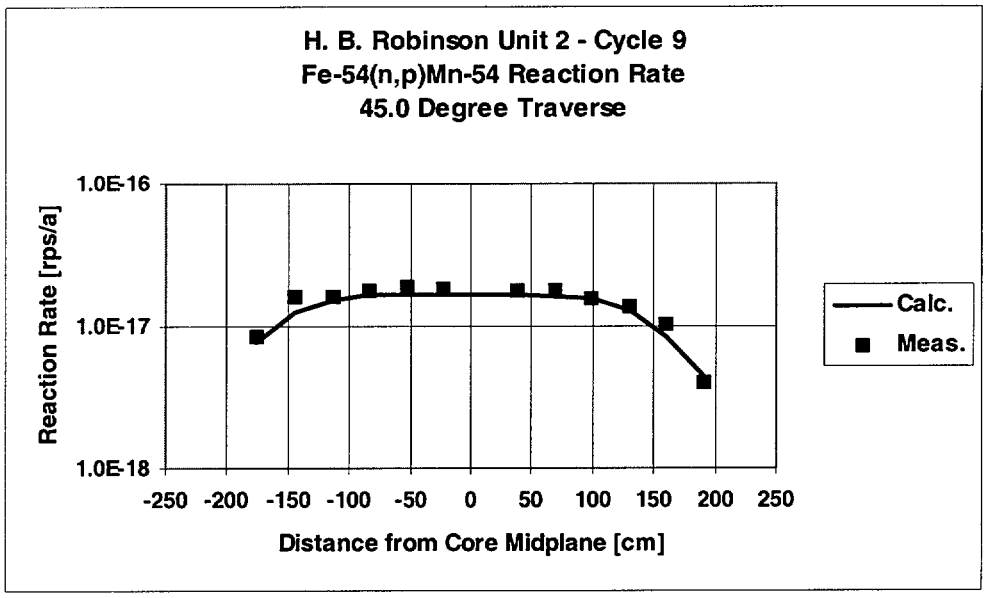

Range of M/C Values 0.91 - 1.26
Average M/C = 1.09
Standard Deviation = 8%

5.0 Analysis of the NUREG/CR-6115 BWR Calculational Benchmark

In support of the development of Regulatory Guide 1.190, the Materials Engineering Branch of the NRC Division of Engineering Technology commissioned Brookhaven National Laboratory (BNL) to develop a set of Pressurized Water Reactor (PWR) and Boiling Water Reactor (BWR) calculational benchmark problems together with solutions determined with the methods described in Regulatory Guide 1.190. Descriptions of the PWR and BWR calculational benchmark problems and the associated calculational results are provided in NUREG/CR-6115[12].

The purpose of this section is to provide a solution to the BWR calculational benchmark described in NUREG/CR-6115 using the Westinghouse fluence methodology. Results of the Westinghouse analysis are compared with the calculational results provided in NUREG/CR-6115 in order to demonstrate the suitability of the Westinghouse methodology for application to the Brunswick Units 1 and 2 fluence analysis.

In the application of the Westinghouse methodology to the fast neutron exposure evaluations for the BWR calculational benchmark problem, discrete ordinates transport calculations were carried out using the same three-dimensional flux synthesis technique used in the Brunswick Units 1 and 2 analysis. The synthesis technique is described as follows:

$$\phi(r,\theta,z) = [\phi(r,\theta)] * [\phi(r,z)]/[\phi(r)]$$

where $\phi(r,\theta,z)$ is the synthesized three-dimensional neutron flux distribution, $\phi(r,\theta)$ is the transport solution in r,θ geometry, $\phi(r,z)$ is the two-dimensional solution for a cylindrical reactor model using the actual axial core power distribution, and $\phi(r)$ is the one-dimensional solution for a cylindrical reactor model using the same source per unit height as that used in the r,θ two-dimensional calculation.

For this analysis, the baseline transport calculations were carried out using the DORT discrete ordinates code Version 3.1[2] and the BUGLE-96 cross-section library[3]. Calculations were performed with both P_5, S_{16} and P_3, S_8. For all locations interior to the reactor vessel the P_5, S_{16} and P_3, S_8 solutions yielded essentially identical results. For the results presented in this section, anisotropic scattering was treated with P_5 legendre expansion and the angular discretization was modeled with an S_{16} order of angular quadrature. The geometric description of the reactor geometry including the compositions of all materials of construction were provided in NUREG/CR-6115. Likewise, the radial and axial distributions of the neutron source for use in the calculational benchmark were given in NUREG/CR-6115.

The r,θ geometric mesh description of the BWR calculational benchmark was comprised of 228 radial by 102 azimuthal intervals. Mesh sizes were chosen to assure that proper convergence of the inner iterations was achieved on a pointwise basis. The pointwise inner iteration flux convergence criterion utilized in the r,θ calculations was set at a value of 0.001. The r,z geometric model consisted of 228 radial by 111 axial intervals and extended from the bottom of the defined problem geometry to an axial elevation approximately three feet above the active fuel region. Since all data comparisons were at locations opposite the active core, the axial geometry was not extended to the top of the defined problem geometry. The one-dimensional, r, geometric model used in the

analysis consisted of the same 228 radial intervals used in the r,z model. In both the r,z and r calculations the pointwise inner iteration flux convergence was also set at a value of 0.001.

Results pertinent to the calculational benchmark are provided in Figures 5-1 through 5-10 and in Tables 5-1 and 5-2. In Figures 5-1 through 5-4, comparisons of the discrete ordinates results from the current analysis to the corresponding discrete ordinates results from the NUREG/CR-6115 solution are provided for the axial elevation of the core midplane. Similar comparisons applicable to the axial location of the maximum fast neutron flux are given in Figures 5-5 through 5-8. In both cases data are provided at a radial location in the downcomer region on the core side of the jet pumps as well as at radial locations corresponding to the 0T, 1/4T, and 3/4T positions within the pressure vessel wall. In Figures 5-9 and 5-10, the discrete ordinates results from the current evaluation are compared with Monte Carlo results from the published NUREG/CR-6115 solution in the downcomer and at the pressure vessel wall. In Tables 5-1 and 5-2, the calculated neutron energy spectra at the downcomer location and within the surveillance capsule are listed for both the current analysis and the NUREG/CR-6115.

In Section 1.4 of NUREG/CR-6115, it is noted that "The calculation-to-calculation benchmark comparisons allow an assessment of the numerical procedures, code implementation, and the various modeling approximations against detailed validated solutions for representative operating configurations. The differences resulting from the uncertainty in the numerical procedures and the modeling of the source and geometry should be small and with present methodologies can be reduced to < (5-10)%." The data comparisons provided in Figures 5-1 through 5-10 and Tables 5-1 and 5-2 are consistent with this statement, thus, demonstrating that the methodology used in the current evaluation provides results applicable to the BWR analysis as defined in the NUREG/CR-6115 problem definition.

Figure 5-1

Fast Neutron Flux (E > 1.0 MeV) as a Function of Azimuthal Angle at the Core Midplane
Downcomer Location R = 278.10, Z =239.93

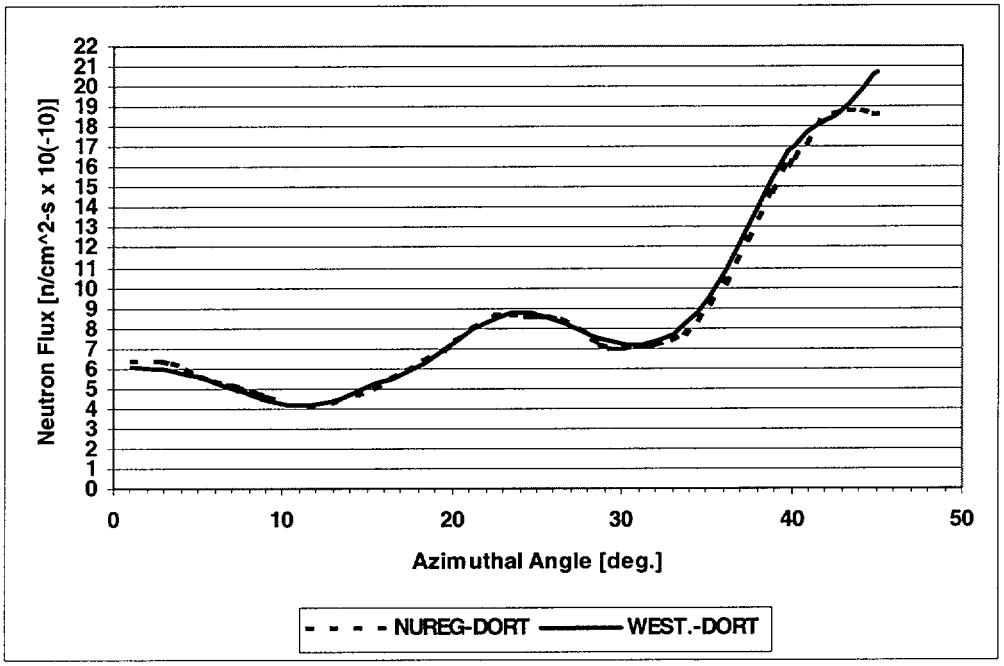

Range of [Westinghouse]/[NUREG] Values 0.93 - 1.11
Average Ratio = 1.01
Standard Deviation = 4%

Note: Comparison ratios and statistical variations are based on the 60 azimuthal data points provided in NUREG/CR-6115.

Figure 5-2

Fast Neutron Flux (E > 1.0 MeV) as a Function of Azimuthal Angle at the Core Midplane
Pressure Vessel 0T Location R = 321.79, Z =239.93

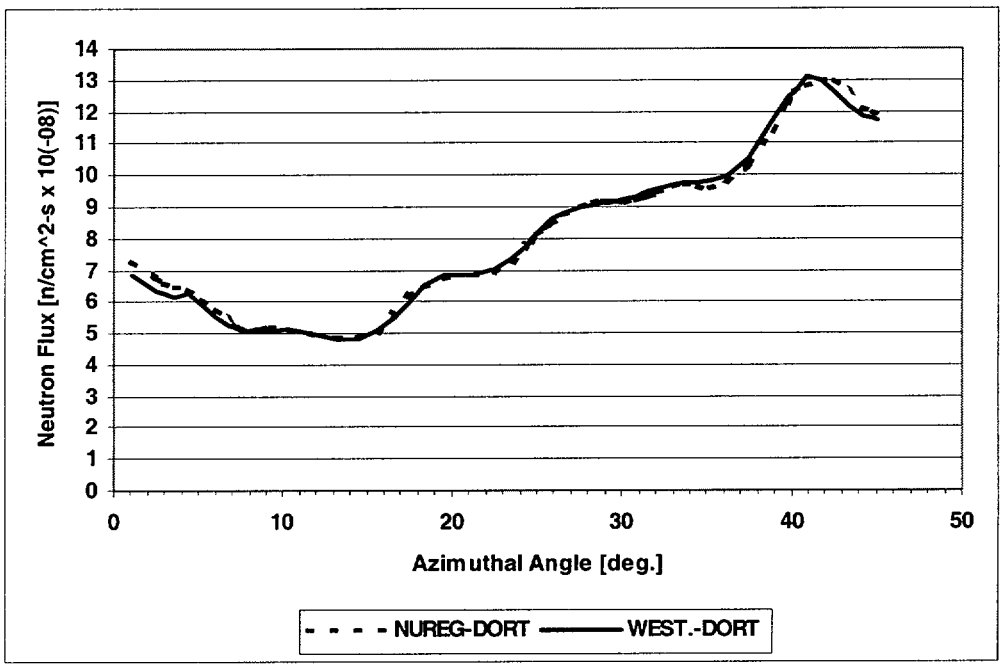

Range of [Westinghouse]/[NUREG] Values 0.93 - 1.03
Average Ratio = 0.99
Standard Deviation = 2%

Note: Comparison ratios and statistical variations are based on the 60 azimuthal data points provided in NUREG/CR-6115.

Figure 5-3

Fast Neutron Flux (E > 1.0 MeV) as a Function of Azimuthal Angle at the Core Midplane
Pressure Vessel 1/4T Location R = 325.82, Z =239.93

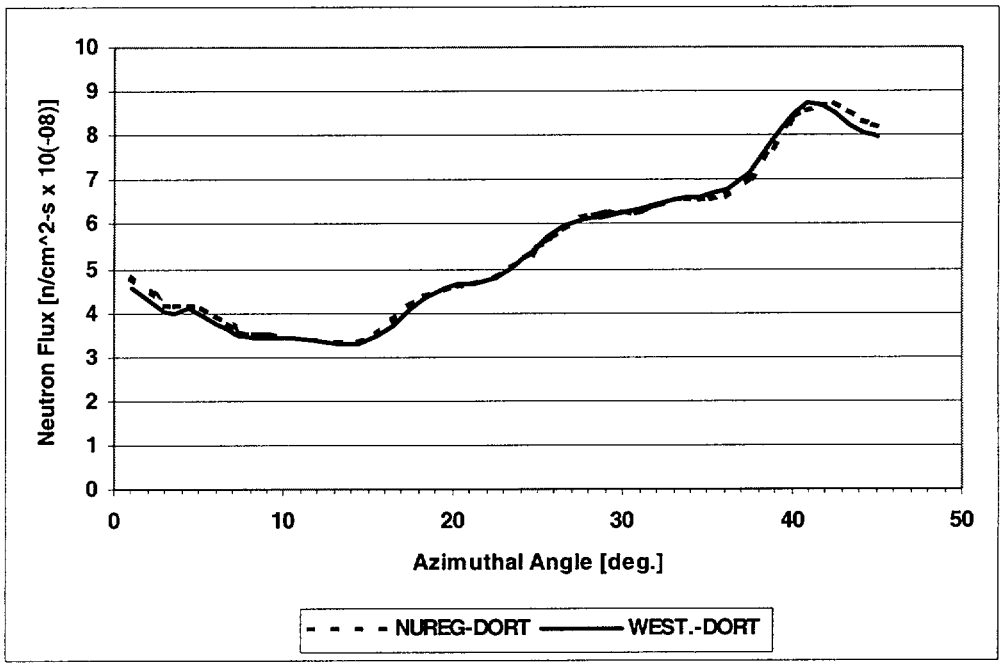

Range of [Westinghouse]/[NUREG] Values 0.94 - 1.02
Average Ratio = 0.99
Standard Deviation = 2%

Note: Comparison ratios and statistical variations are based on the 60 azimuthal data points provided in NUREG/CR-6115.

Figure 5-4

Fast Neutron Flux (E > 1.0 MeV) as a Function of Azimuthal Angle at the Core Midplane
Pressure Vessel 3/4T Location R = 333.88, Z =239.93

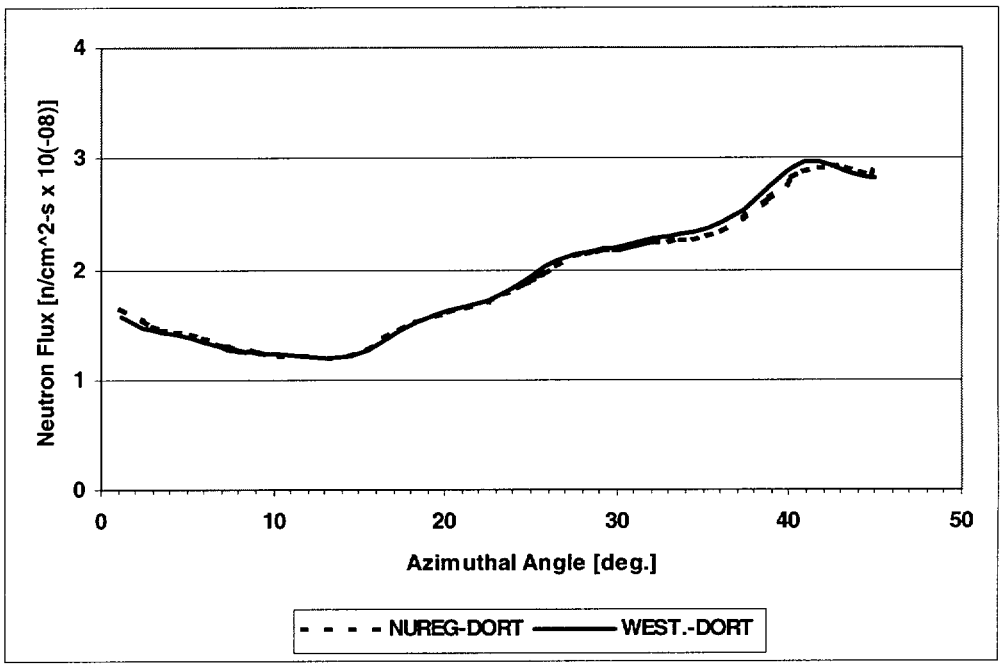

Range of [Westinghouse]/[NUREG] Values 0.96 - 1.04
Average Ratio = 1.00
Standard Deviation = 2%

Note: Comparison ratios and statistical variations are based on the 60 azimuthal data points provided in NUREG/CR-6115.

Figure 5-5

Maximum Fast Neutron Flux (E > 1.0 MeV) as a Function of Azimuthal Angle
Downcomer Location R = 278.10, Z =306.61

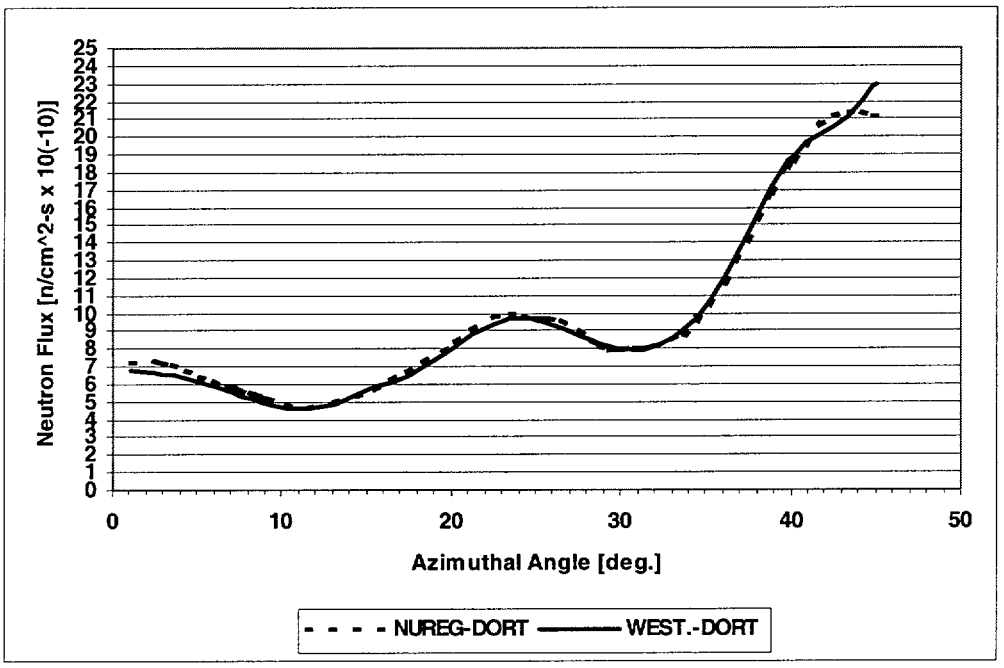

Range of [Westinghouse]/[NUREG] Values 0.91 - 1.08
Average Ratio = 0.98
Standard Deviation = 4%

Note: Comparison ratios and statistical variations are based on the 60 azimuthal data points provided in NUREG/CR-6115.

Figure 5-6

Maximum Fast Neutron Flux (E > 1.0 MeV) as a Function of Azimuthal Angle
Pressure Vessel 0T Location R = 321.79, Z =306.61

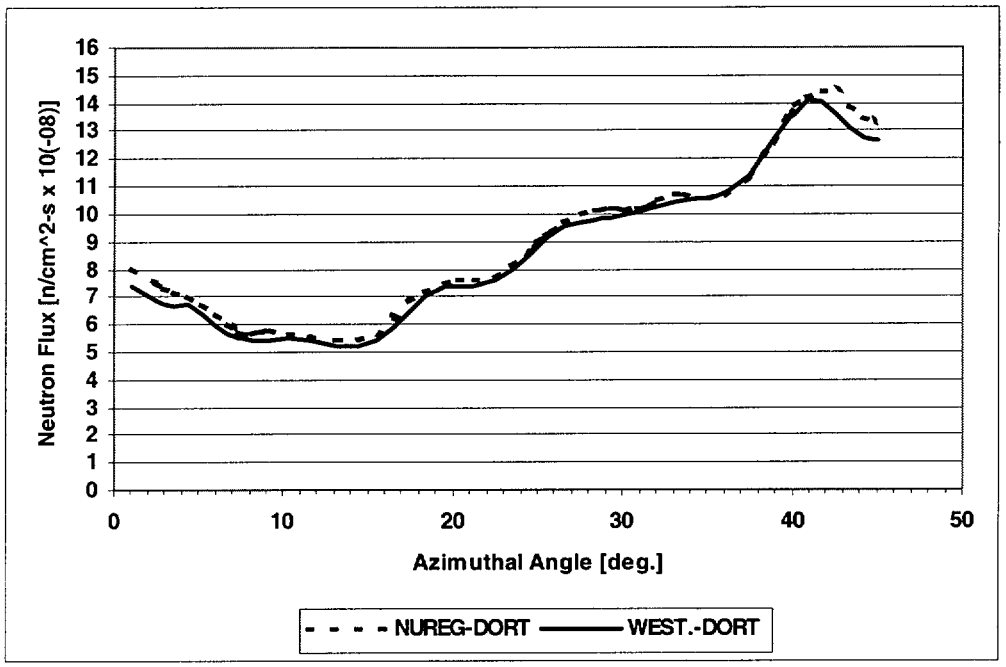

Range of [Westinghouse]/[NUREG] Values 0.91 - 1.01
Average Ratio = 0.97
Standard Deviation = 2%

Note: Comparison ratios and statistical variations are based on the 60 azimuthal data points provided in NUREG/CR-6115.

Figure 5-7

Maximum Fast Neutron Flux (E > 1.0 MeV) as a Function of Azimuthal Angle
Pressure Vessel 1/4T Location R = 325.82, Z =306.61

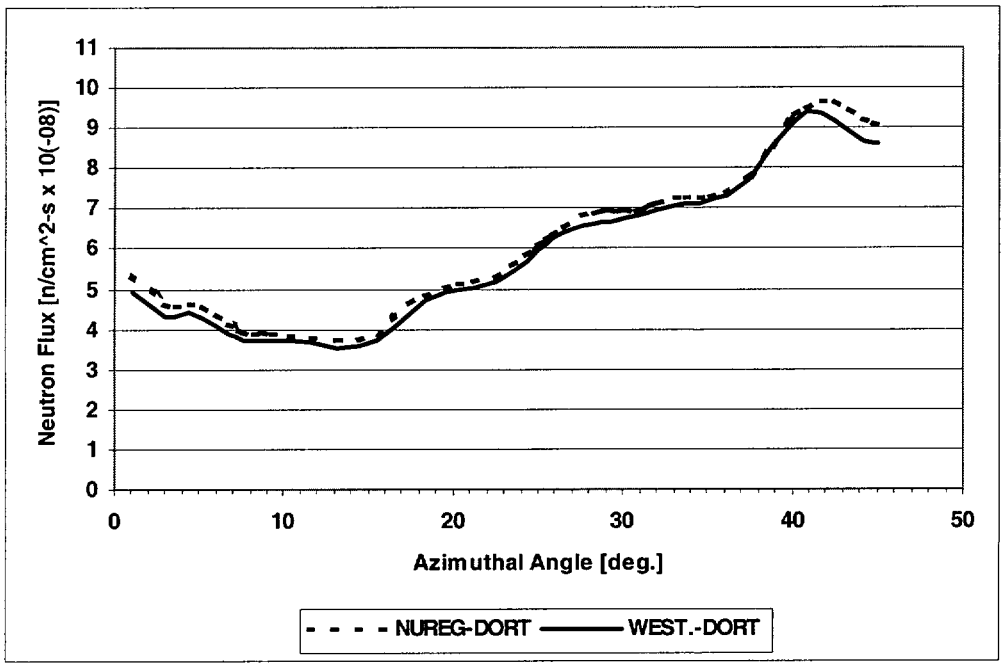

Range of [Westinghouse]/[NUREG] Values 0.92 - 1.00
Average Ratio = 0.96
Standard Deviation = 2%

Note: Comparison ratios and statistical variations are based on the 60 azimuthal data points provided in NUREG/CR-6115.

Figure 5-8

Maximum Fast Neutron Flux (E > 1.0 MeV) as a Function of Azimuthal Angle
Pressure Vessel 3/4T Location R = 333.88, Z =306.61

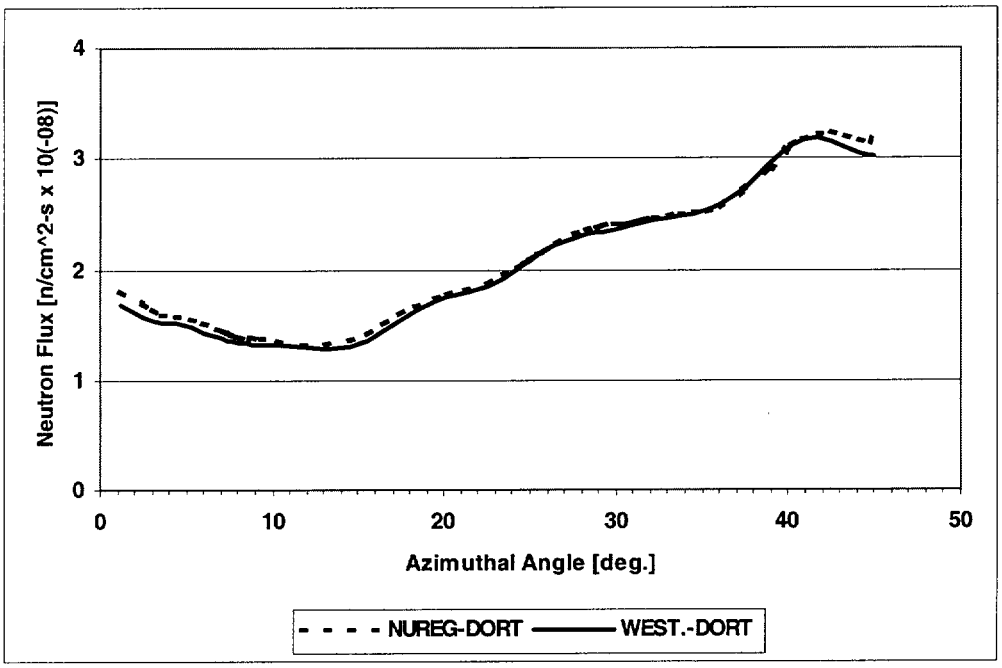

Range of [Westinghouse]/[NUREG] Values 0.93 - 1.01
Average Ratio = 0.98
Standard Deviation = 2%

Note: Comparison ratios and statistical variations are based on the 60 azimuthal data points provided in NUREG/CR-6115.

Figure 5-9

Fast Neutron Flux (E > 1.0 MeV) as a Function of Azimuthal Angle at the Core Midplane
Downcomer Location R = 278.10, Z =239.93

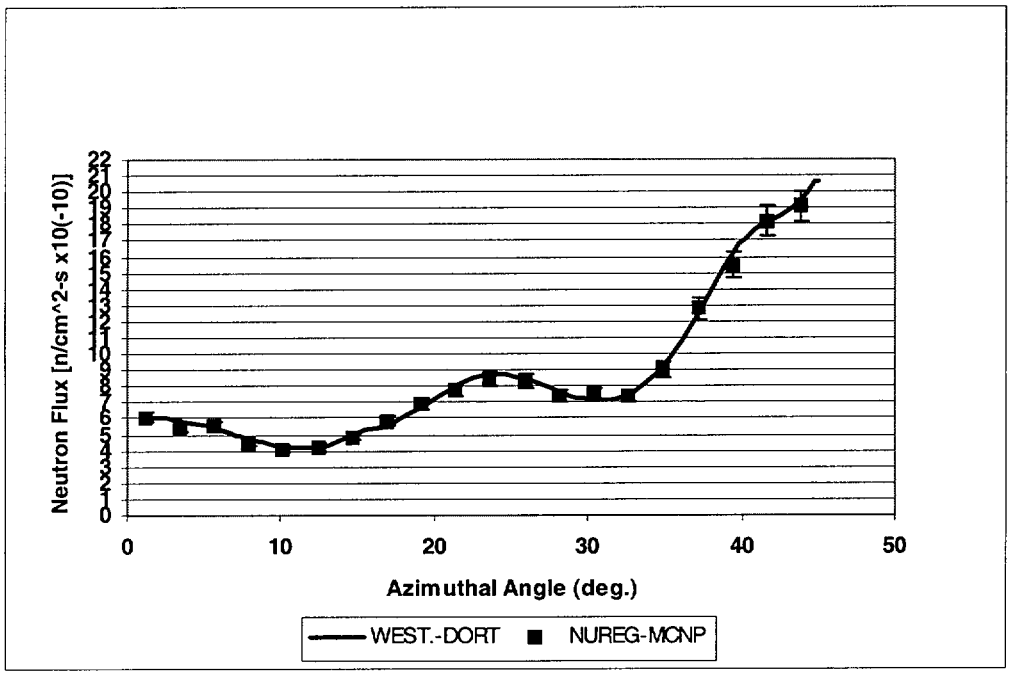

Range of [Westinghouse]/[NUREG] Values 0.95 - 1.08
Average Ratio = 1.01
Standard Deviation = 3%

Note: Comparison ratios and statistical variations are based on the 20 azimuthal data points provided in NUREG/CR-6115.

Figure 5-10

Fast Neutron Flux (E > 1.0 MeV) as a Function of Azimuthal Angle at the Core Midplane
Pressure Vessel Wall Location R = 323.14, Z =239.93

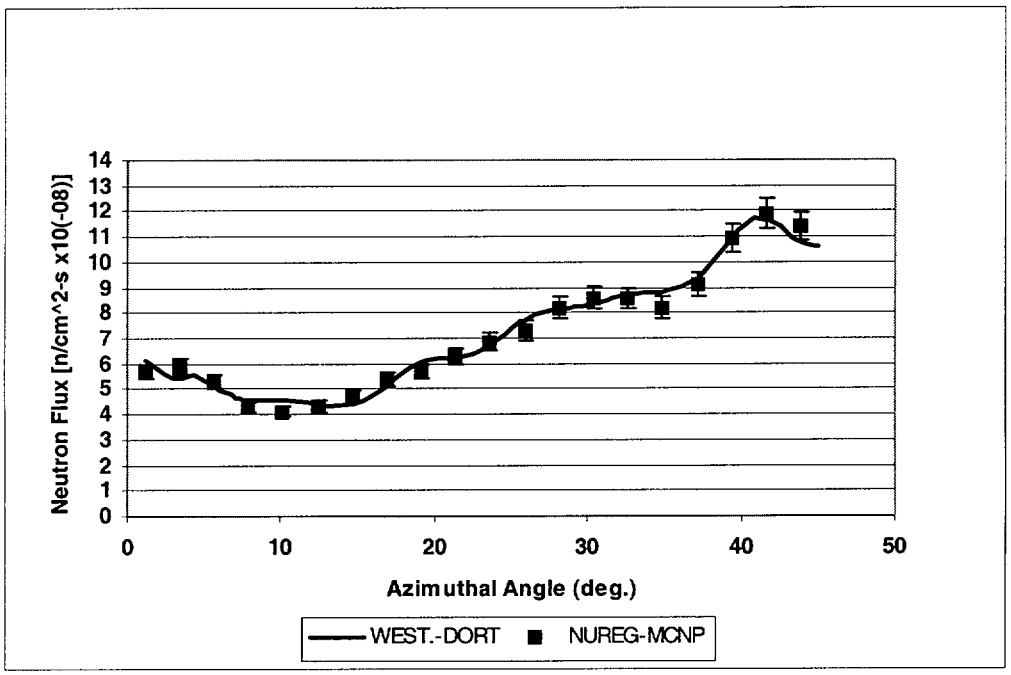

Range of [Westinghouse]/[NUREG] Values 0.92 - 1.12
Average Ratio = 1.01
Standard Deviation = 5%

Note: Comparison ratios and statistical variations are based on the 20 azimuthal data points provided in NUREG/CR-6115.

Table 5-1

Comparison of the Calculated Neutron Spectrum at the Downcomer Location
R = 278.10 cm, Z = 306.61 cm., θ = 23.5°

BUGLE Energy Group	Neutron Flux [n/cm^2-s]		[West]/[NUREG]
	Westinghouse	NUREG	
1	3.21e+07	3.06e+07	1.048
2	1.05e+08	9.94e+07	1.051
3	4.55e+08	4.35e+08	1.048
4	9.09e+08	8.70e+08	1.045
5	1.65e+09	1.58e+09	1.043
6	4.43e+09	4.24e+09	1.043
7	6.69e+09	6.45e+09	1.038
8	1.22e+10	1.19e+10	1.029
9	8.48e+09	8.29e+09	1.023
10	5.85e+09	5.72e+09	1.023
11	6.42e+09	6.29e+09	1.021
12+13	3.88e+09	3.79e+09	1.022
14	3.80e+09	3.72e+09	1.020
15	9.04e+09	8.90e+09	1.016
16	9.04e+09	8.93e+09	1.012
17	1.21e+10	1.20e+10	1.008
18	1.59e+10	1.60e+10	0.999
19	1.00e+10	1.00e+10	0.998
20	5.75e+09	5.75e+09	0.999
21	1.06e+10	1.07e+10	0.994
22	9.44e+09	9.48e+09	0.996
23	1.05e+10	1.05e+10	0.998
24	8.23e+09	8.28e+09	0.994
25	1.52e+10	1.52e+10	1.000
26	1.28e+10	1.28e+10	0.999
27	1.09e+10	1.09e+10	0.999
28	9.61e+09	9.60e+09	1.001
29	4.48e+09	4.48e+09	1.002
30	3.48e+09	3.47e+09	1.003
31	1.28e+10	1.28e+10	1.000
32	1.70e+09	1.70e+09	1.000
33	6.23e+09	6.21e+09	1.004
34	1.21e+10	1.20e+10	1.005
35	1.18e+10	1.17e+10	1.005
36	1.18e+10	1.17e+10	1.006
37	1.97e+10	1.95e+10	1.008
38	1.19e+10	1.18e+10	1.009
39	1.20e+10	1.19e+10	1.010
40	1.61e+10	1.60e+10	1.011
41	2.04e+10	2.01e+10	1.013
42	1.23e+10	1.22e+10	1.014
43	1.73e+10	1.71e+10	1.013
44	1.37e+10	1.36e+10	1.004
45	1.41e+10	1.50e+10	0.941
46+47	8.85e+11	7.68e+11	1.151

Table 5-2

Comparison of the Calculated Neutron Spectrum at the Capsule Location
R = 319.20 cm, Z = 306.61 cm., θ = 3°

BUGLE Energy Group	Neutron Flux [n/cm²-s]		[West]/[NUREG]
	Westinghouse	NUREG	
1	1.19e+06	1.20e+06	0.989
2	3.21e+06	3.22e+06	0.997
3	1.07e+07	1.07e+07	0.999
4	1.84e+07	1.84e+07	1.002
5	2.72e+07	2.72e+07	1.000
6	6.53e+07	6.55e+07	0.997
7	7.89e+07	8.02e+07	0.984
8	1.12e+08	1.15e+08	0.973
9	6.92e+07	7.13e+07	0.971
10	4.56e+07	4.75e+07	0.961
11	4.84e+07	5.03e+07	0.963
12+13	2.82e+07	2.96e+07	0.951
14	2.78e+07	2.94e+07	0.948
15	7.26e+07	7.66e+07	0.947
16	7.24e+07	7.86e+07	0.922
17	9.80e+07	1.04e+08	0.943
18	1.48e+08	1.57e+08	0.942
19	8.79e+07	9.34e+07	0.941
20	4.58e+07	4.87e+07	0.940
21	1.13e+08	1.36e+08	0.832
22	8.67e+07	8.96e+07	0.968
23	1.04e+08	1.15e+08	0.905
24	8.92e+07	1.06e+08	0.844
25	1.14e+08	1.14e+08	0.997
26	1.06e+08	1.21e+08	0.874
27	7.48e+07	8.91e+07	0.840
28	5.66e+07	5.37e+07	1.054
29	2.06e+07	1.90e+07	1.087
30	1.30e+07	1.08e+07	1.202
31	1.91e+07	2.58e+07	0.741
32	1.41e+07	1.38e+07	1.022
33	2.51e+07	3.13e+07	0.803
34	5.36e+07	4.57e+07	1.173
35	6.99e+07	7.64e+07	0.915
36	6.55e+07	6.40e+07	1.023
37	9.56e+07	9.44e+07	1.013
38	5.52e+07	5.65e+07	0.978
39	5.68e+07	5.82e+07	0.976
40	7.49e+07	7.71e+07	0.972
41	9.02e+07	9.26e+07	0.974
42	5.15e+07	5.28e+07	0.975
43	6.43e+07	6.63e+07	0.969
44	4.51e+07	4.76e+07	0.947
45	3.51e+07	4.15e+07	0.847
46+47	7.71e+08	6.81e+08	1.132

6.0 Brunswick Units 1 and 2 Operating Plant Comparisons

Section 1.4.2.1 of Regulatory Guide 1.190 states that *"Comparisons of measurements and calculations must be performed for the specific reactor being analyzed or for reactors of similar design. Plant specific measurements have the advantage of including the as-built materials and geometry and the actual reactor operating conditions. An especially accurate determination of the fluence can be obtained when both in-vessel and cavity dosimetry are available."*

In the case of Brunswick Units 1 and 2, a single in-vessel surveillance capsule has been withdrawn from the 30 degree azimuthal location in each unit. At Brunswick Unit 1, the capsule was irradiated during fuel cycles 1 through 8, while for Brunswick Unit 2, the irradiation period spanned fuel cycles 1 through 11. In both reactors, the 30 degree surveillance capsule was located behind a jet pump.

In addition, to these in-vessel capsules irradiated as a part of the reactor vessel materials surveillance program, an ex-vessel dosimetry program was also carried out during the sixth fuel cycle at each unit.[10,11] The ex-vessel measurement program included axial traverse data at several azimuthal angles in the reactor cavity located between the pressure vessel insulation and the sacrificial shield. These traverses spanned the height of the active fuel zone. Since the maximum fluence on the Brunswick Units 1 and 2 reactor pressure vessels occurs at the 45 degree azimuth between the jet pumps, axial measurement traverses were taken along each of the four minor axes (45º, 135º, 225º, and 315º).

Results of the analysis of the Brunswick Units 1 and 2 dosimetry are provided in Tables 6-1 through 6-3 and in Figures 6-1 through 6-9. In Tables 6-1 and 6-2, the current calculated results are compared with the measured sensor reaction rates at the 30 degree in-vessel surveillance capsule location for Brunswick Units 1 and 2, respectively. Also given in Tables 6-1 and 6-2 are the corresponding ratios of measured to calculated reaction rates, (M/C), for each sensor reaction.

In Figures 6-1 through 6-9, the current calculated results are compared to the ex-vessel iron gradient measurements obtained at Unit 1 (Figures 6-1 through 6-4), and Unit 2 (Figures 6-5 through 6-9). A summary of the average M/C ratio derived from each of these nine data traverses is provided in Table 6-3.

An examination of Table 6-3 shows that, considering the Unit 1 and Unit 2 data as a single data base, that the in-vessel M/C ratios range from 1.11 to 1.15 for the two sample set. The overall average of this in-vessel data is 1.13 with an associated standard deviation of 13%. In the case of the ex-vessel comparisons, the average M/C ratios for the nine sample set range from 0.97 to 1.19. The overall average of the ex-vessel data is 1.05 with an associated standard deviation of 10%. Both the ex-vessel and in-vessel data sets fall within the 20% criterion specified in Section 1.4.3 of Regulatory Guide 1.190.

In addition to the M/C comparisons given in Table 6-3, a qualitative examination of Figures 6-1 through 6-9 indicates that, as was the case with the H. B. Robinson Benchmark calculations, the three-dimensional synthesis approach results in a reasonable calculation of the axial distribution of neutron fluence over the active core

height. This agreement, in turn, indicates that the axial power distributions and void fraction variations are being treated properly in the transport calculations.

Table 6-1

Reaction Rate M/C Comparisons for the Brunswick Unit 1
30 Degree In- Vessel Capsule - Cycles 1-8

	Calculated	Measured	M/C
$^{63}Cu(n,\alpha)^{60}Co$	3.12e-18	3.99e-18	1.28
$^{54}Fe(n,p)^{54}Mn$	1.99e-16	2.16e-16	1.08
$^{58}Ni(n,p)^{58}Co$	2.55e-16	2.48e-16	0.97
Average			1.11
% Standard Deviation			14

Table 6-2

Reaction Rate M/C Comparisons for the Brunswick Unit 2
30 Degree In- Vessel Capsule - Cycles 1-11

	Calculated	Measured	M/C
$^{54}Fe(n,p)^{54}Mn$	1.97e-16	2.45e-16	1.24
$^{58}Ni(n,p)^{58}Co$	2.52e-16	2.68e-16	1.06
Average			1.15
% Standard Deviation			11

Table 6-3

Summary of Multiple Foil and Gradient Chain M/C Ratios

Data Set	Number Of Samples	Average M/C	Std. Dev. (%)
30 Deg. In-Vessel Foil Set - Unit 1	9	1.11	14
30 Deg. In-Vessel Foil Set - Unit 2	6	1.15	11
14 Deg. Ex-Vessel Gradient – Unit 1	13	1.01	9
23 Deg. Ex-Vessel Gradient – Unit 1	11	0.97	14
36 Deg. Ex-Vessel Gradient – Unit 1	12	1.11	7
45 Deg. Ex-Vessel Gradient – Unit 1	52	0.99	10
0 Deg. Ex-Vessel Gradient – Unit 2	10	1.00	12
12 Deg. Ex-Vessel Gradient – Unit 2	14	1.19	11
15 Deg. Ex-Vessel Gradient – Unit 2	28	1.10	7
23 Deg. Ex-Vessel Gradient – Unit 2	14	1.05	11
45 Deg. Ex-Vessel Gradient – Unit 2	51	1.04	10

Figure 6-1

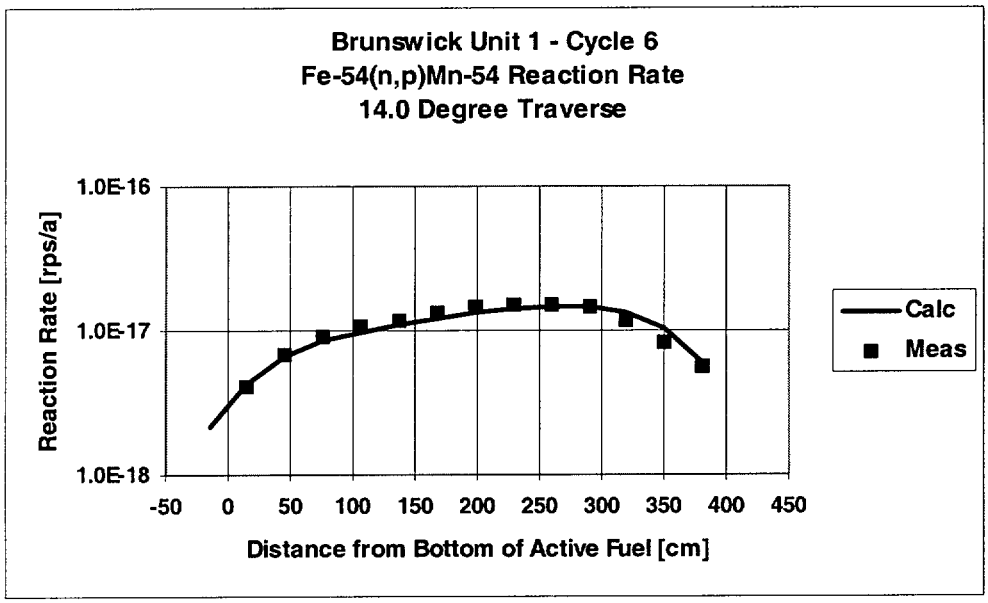

Range of M/C Values 0.78 - 1.10
Average M/C = 1.01
Standard Deviation = 9%

Figure 6-2

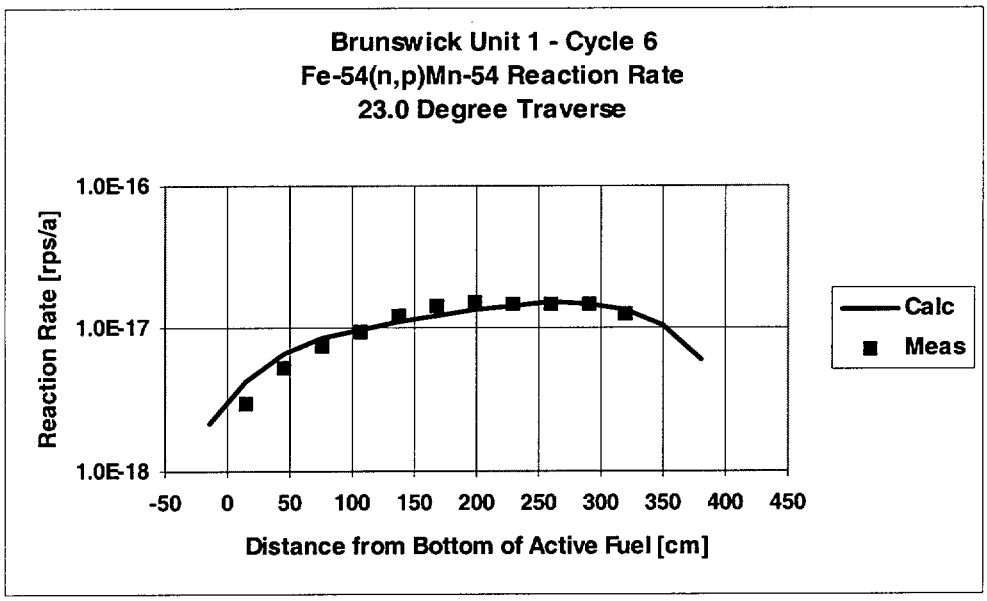

Range of M/C Values 0.70 - 1.16
Average M/C = 0.97
Standard Deviation = 14%

Figure 6-3

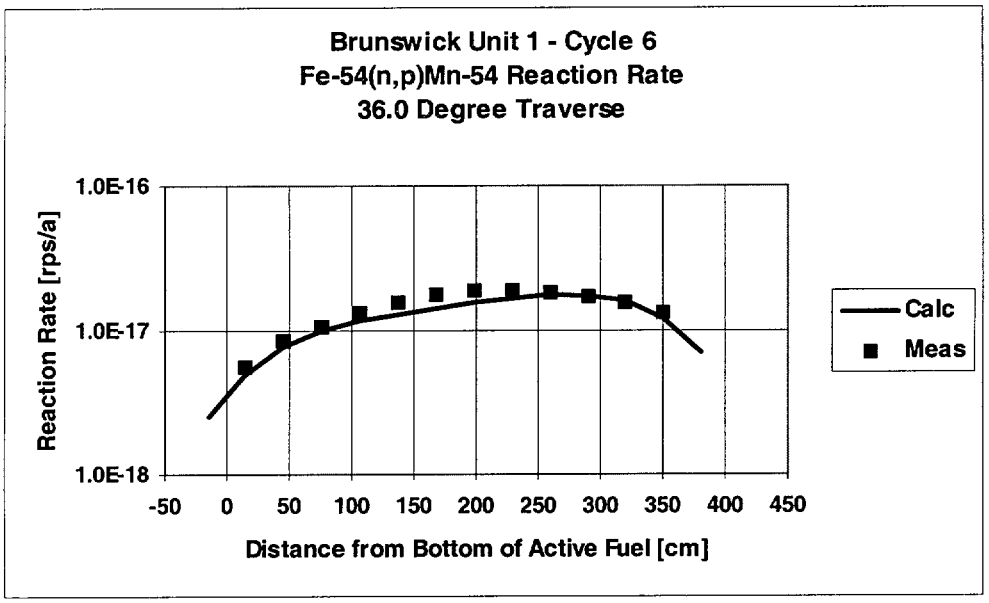

Range of M/C Values 0.98 - 1.25
Average M/C = 1.11
Standard Deviation = 7%

Figure 6-4

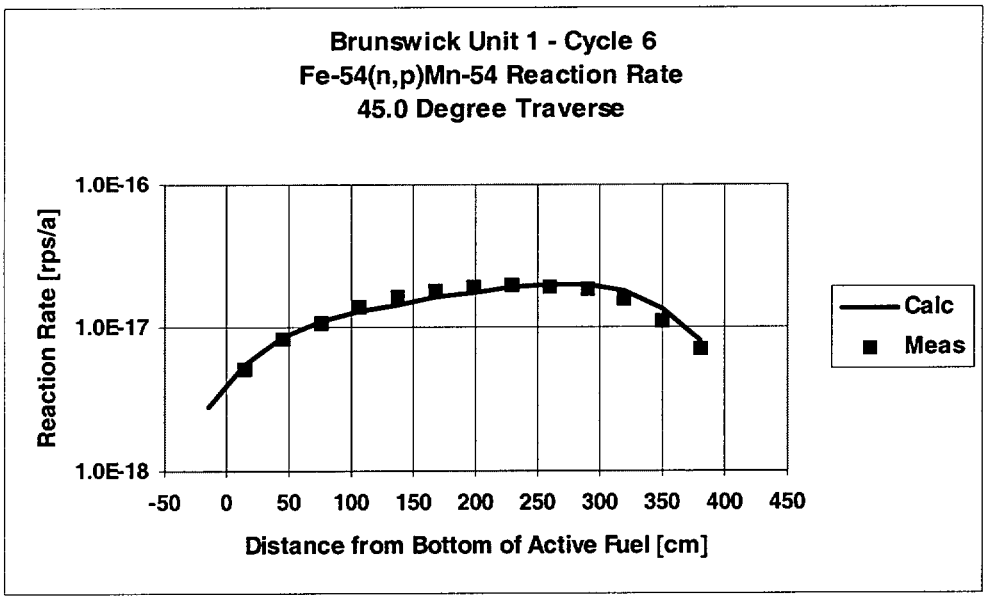

Range of M/C Values 0.83 - 1.13
Average M/C = 0.99
Standard Deviation = 10%

Figure 6-5

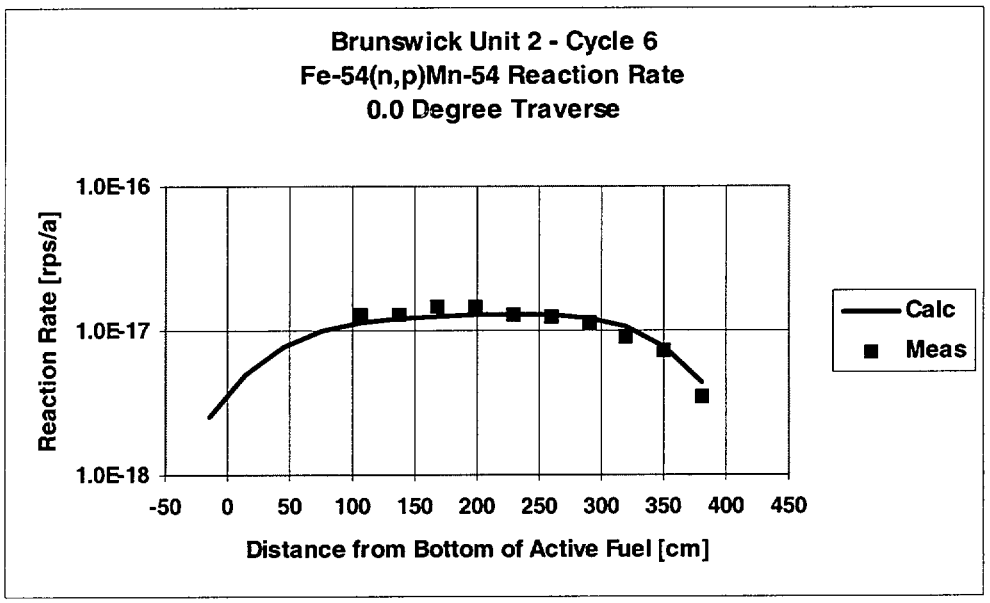

Range of M/C Values 0.80 - 1.15
Average M/C = 1.00
Standard Deviation = 12%

Figure 6-6

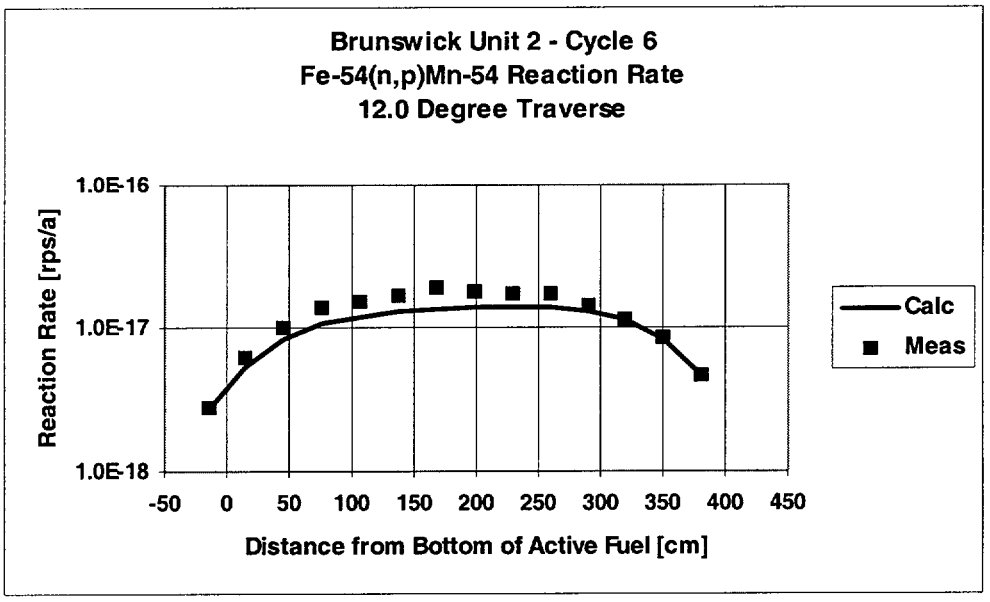

Range of M/C Values 0.99 - 1.41
Average M/C = 1.19
Standard Deviation = 11%

Figure 6-7

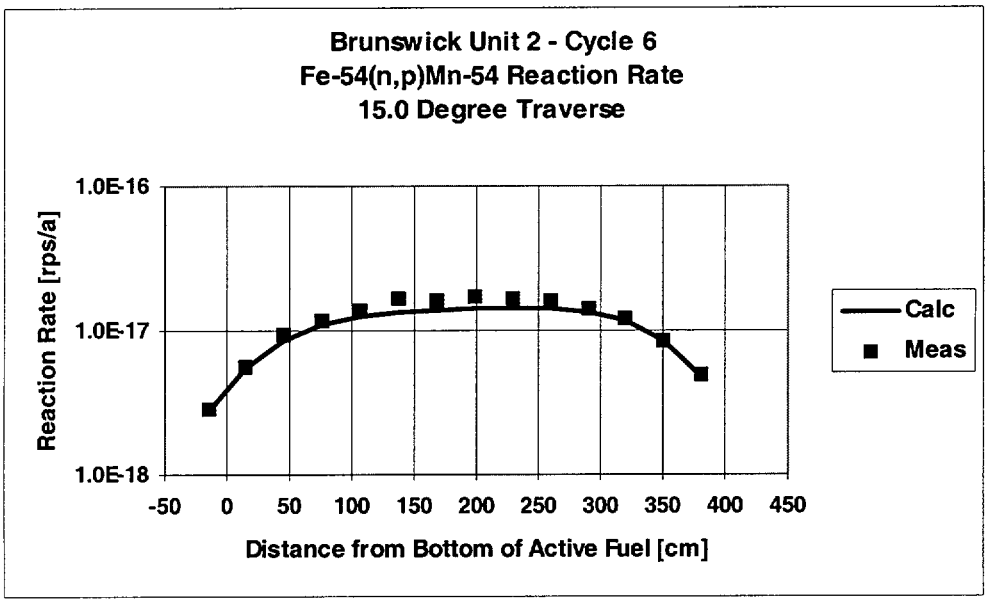

Range of M/C Values 0.98 - 1.25
Average M/C = 1.10
Standard Deviation = 7%

Figure 6-8

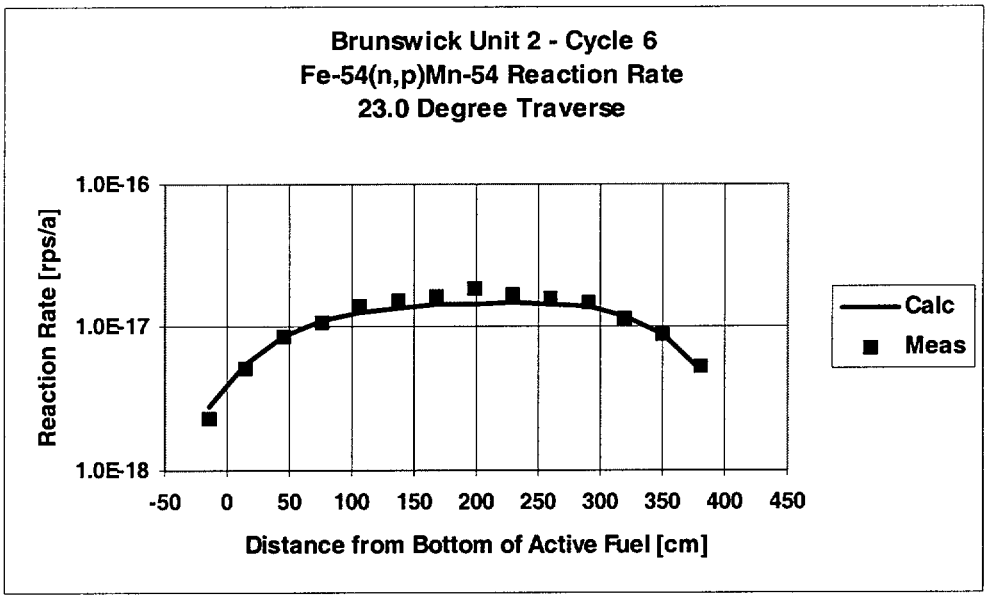

Range of M/C Values 0.83 - 1.28
Average M/C = 1.05
Standard Deviation = 11%

Figure 6-9

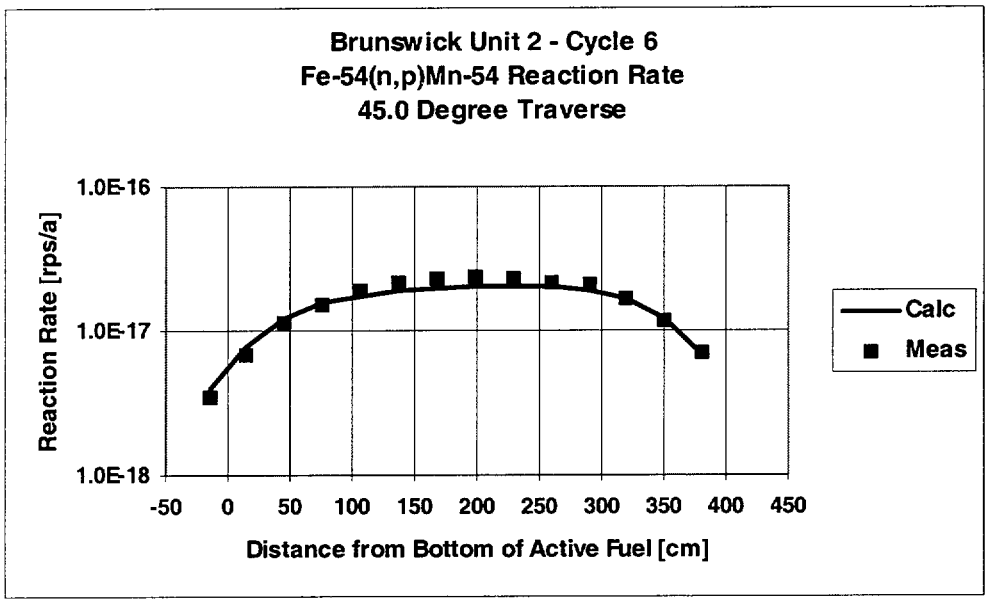

Range of M/C Values 0.88 - 1.16
Average M/C = 1.04
Standard Deviation = 10%

7.0 Sensitivity Studies

The uncertainty associated with the calculated neutron exposure for Brunswick Units 1 and 2 is based on the recommended approach provided in Regulatory Guide 1.190. In particular, the qualification of the methodology used in exposure evaluations was carried out in the following four stages:

1 - Comparisons of calculations with benchmark measurements from the Pool Critical Assembly (PCA) simulator at the Oak Ridge National Laboratory (ORNL).

2 - Comparison of calculations with surveillance capsule and reactor cavity measurements from the H. B. Robinson power reactor benchmark experiment.

3 - An analytical sensitivity study addressing the uncertainty components resulting from important input parameters applicable to the plant specific transport calculations used in the neutron exposure assessments.

4 - Comparisons of the calculations with available dosimetry results from measurement programs carried out at the Brunswick Units 1 and 2 reactors.

The first phase of the methods qualification addressed the adequacy of basic transport calculation and dosimetry evaluation techniques and associated cross-sections. This, phase, however, did not test the accuracy of commercial core neutron source calculations nor did it address uncertainties in operational and geometric variables that impact power reactor calculations. The second phase of the qualification addressed uncertainties that are primarily methods related and would tend to apply generically to all fast neutron exposure evaluations. The third phase of the qualification identified the potential uncertainties introduced into the overall evaluation due to calculational methods approximations as well as to a lack of knowledge relative to various plant specific parameters. The overall calculational uncertainty was established from the results of these three phases of the methods qualification.

The comparison of the calculated results with the available plant specific dosimetry results was used solely to demonstrate the adequacy of the transport calculations and to confirm the uncertainty estimates associated with the analytical results. The comparison was used only as a check and was not used to bias the final results in any way.

The following summarizes the uncertainties associated with the Brunswick Units 1 and 2 neutron exposure calculations:

PCA Benchmark Comparisons	3%
H. B. Robinson Benchmark Comparisons	3%
Analytical Sensitivity Studies	
Internals Dimensions	3%
Vessel Inner Radius	5%
Water Temperature	4%
Peripheral Assembly Source Strength	5%
Axial Power Distribution	5%
Peripheral Assembly Burnup	2%
Spatial Distribution of the Source	4%
Other Factors	5%

The category designated "Other Factors" is intended to attribute an additional uncertainty to other geometrical or operational variables that individually have an insignificant impact on the overall uncertainty, but collectively should be accounted for in the assessment. In the overall uncertainty evaluation, these uncertainty components are considered to be at the 1σ level.

When the uncertainty components tabulated above are combined in quadrature, the resultant uncertainty in the Brunswick Units 1 and 2 calculated exposure levels is estimated to be 14% at the 1σ level.

The comparisons of the transport calculation results with data from the Brunswick Units 1 and 2 in-vessel and ex-vessel measurement programs support the fourth phase of the methods qualification and demonstrate that the requirements of Regulatory Guide 1.190 are met.

In addition to the sensitivity analyses discussed above, two additional studies were carried out to address issues pertinent to the Brunswick calculations. The first was an assessment of the impact of jet pump modeling on the calculated exposure of the reactor pressure vessel. The second was a study of the effect of P_L scattering order and S_n quadrature on the ex-vessel dosimetry calculations.

The jet pump study was carried out by completing an r,θ calculation for a single cycle with and without the jet pumps included in the analytical model. The results of this evaluation are given in Table 7-1. The data included in Table 7-1 show that the maximum effect of 18% occurs directly behind the jet pump structure located on the core cardinal axes. On the other hand, at the location of the maximum vessel exposure along the core minor axes, the impact of the jet pump modeling is negligible.

Since prior experience in analyzing ex-vessel dosimetry for pressurized water reactors has indicated that the use of a P_5, S_{16} approximation will, in some cases, improve comparisons with measurements, cycle 6 for both Brunswick Units 1 and 2 were re-evaluated using the higher order approximations. Relative to the baseline P_3, S_8 calculations, there were negligible changes at locations internal to the pressure vessel, However, at the locations of the ex-vessel dosimetry, the calculated reaction rates were

increased by 4-5% depending on location and the energy response of the sensor. Thus, while not impacting pressure vessel exposure projections, the use of the higher order approximations did improve the comparison between the calculations and the ex-vessel measurements.

Table 7-1

Effect of Jet Pump Modeling at the Pressure Vessel Inner Radius

Azimuthal Location [Deg.]	Calculated Flux With Jet Pumps	Calculated Flux Without Jet Pumps	With/Without
0	6.41e+08	7.77e+08	0.82
12	9.22e+08	9.59e+08	0.96
14	9.82e+08	1.00e+09	0.98
22	9.40e+08	1.00e+09	0.94
37	1.13e+09	1.24e+09	0.91
45	1.44e+09	1.46e+09	0.99

Note: Comparisons are based on an r,θ calculation of the fast neutron flux (E > 1.0 MeV) for Brunswick Unit 1, cycle 6.

8.0 References

1. Regulatory Guide 1.190, "Calculational and Dosimetry Methods for Determining Pressure Vessel Neutron Fluence," U. S. Nuclear Regulatory Commission, Office of Nuclear Regulatory Research, March 2001.

2. RSICC Computer Code Collection CCC-650, "DOORS 3.1, One-, Two-, and Three-Dimensional Discrete Ordinates Neutron/Photon Transport Code System," August 1996.

3. RSICC Data Library Collection DLC-185, "BUGLE-96, Coupled 47 Neutron, 20 Gamma-Ray Group Cross-Section Library Derived from ENDF/B-VI for LWR Shielding and Pressure Vessel Dosimetry Applications," March 1996.

4. RSICC Data Library Collection DLC-178, "SNLRML Recommended Dosimetry Cross-Section Compendium," July 1994.

5. I. Remec and F. B. K. Kam, "Pool Critical Assembly Pressure Vessel Benchmark," NUREG/CR-6454 (ORNL/TM-13205), July 1997.

6. W. N. McElroy, et al, "LWR Pressure Vessel Surveillance Dosimetry Improvement Program: PCA Experiments and Blind Test," NUREG/CR-1861 (HEDL-TME 80-87), July 1981.

7. W. N. McElroy, et al, "LWR Pressure Vessel Surveillance Dosimetry Improvement Program: PCA Experiments, Blind Test, and Physics-Dosimetry Support for the PSF Experiments," NUREG/CR-3318 (HEDL-TME 84-1), September 1984.

8. I. Remec and F. B. K. Kam, "H. B. Robinson Pressure Vessel Benchmark," NUREG/CR-6453 (ORNL/TM-13204), February 1998.

9. E. P. Lippincott, et al, "Evaluation of Surveillance Capsule and Reactor Cavity Dosimetry from H. B. Robinson Unit 2, Cycle 9," NUREG/CR-4576 (WCAP-11104), February 1987.

10. S. L. Anderson, "Reactor Cavity Neutron Measurement Program for Carolina Power and Light Company Brunswick Unit 1," WCAP-13183, January 1992.

11. S. L. Anderson, E. P. Lippincott, and J. Sejvar, "Reactor Cavity Neutron Dosimetry Program for Brunswick Unit 2," WCAP-10903, December 1986.

12. J. F. Carew, et al, "PWR and BWR Pressure Vessel Fluence Calculation Benchmark Problems and Solutions," NUREG/CR-6115, September 2001.

Summary of Compliance with the Regulatory Positions Specified in Regulatory Guide 1.190

FLUENCE CALCULATION METHODS

Regulatory Position	NRC Staff Position	Westinghouse Approach
1.3	**Fluence Determination**. Absolute fluence calculations, rather than extrapolated fluence measurements, must be used for the fluence determination.	Fluence evaluations are based on absolute calculations using the discrete ordinates transport method and the 2D/3D synthesis technique described in Section 1.3.4 of Regulatory Guide 1.190.
1.1.1	**Modeling Data**. The calculation modeling (geometry, materials, etc.) should be based on documented and verified plant specific data.	The calculation model is based on nominal dimensions obtained from plant specific design drawings. System operating temperatures and, hence coolant densities are treated on a fuel cycle specific basis.
1.1.2	**Nuclear Data**. The latest version of the Evaluated Nuclear Data File (ENDF/B) should be used for determining cross-sections. Cross-section sets based on earlier or equivalent nuclear data sets that have been thoroughly benchmarked are also acceptable. When the recommended cross-section data change, the effect of these changes on licensee specific methodology must be evaluated and the fluence estimates updated when the effects are significant.	Discrete ordinates calculations make use of the BUGLE-96 ENDF/B-VI based cross-section library. The BUGLE-96 library is a 67 group (47 neutron, 20 gamma ray) data set produced specifically for light water reactor (LWR) applications by the Oak Ridge National Laboratory (ORNL). ENDF/B-VI represents the latest version of the Evaluated Nuclear Data File (ENDF/B).
1.1.2	**Cross-Section Angular Representation**. In discrete ordinates transport calculations, a P_3 angular decomposition of the scattering cross-sections (at a minimum) must be employed.	A P_3 scattering approximation was used in all of the cycle specific fluence calculations. A P_5 calculation was also performed as a part of the analytical uncertainty study and tested against ex-vessel measurements.

Regulatory Position	NRC Staff Position	Westinghouse Approach
1.1.2	**Cross-Section Group Collapsing.** The adequacy of the collapsed job library must be demonstrated by comparing calculations for a representative configuration performed with both the master library and the job library.	The BUGLE-96 library is itself a collapsed job library. The testing required by this Staff Position was performed by ORNL prior to the general release of the BUGLE-96 library and is included in the documentation package accompanying the library (RSIC Data Library Collection DLC-185).
1.2	**Neutron Source.** The core neutron source should account for local fuel isotopics and, where appropriate, the effects of moderator density. The neutron source normalization and energy dependence must account for the fuel exposure dependence of the fission spectra, the number of neutrons produced per fission, and the energy released per fission.	Core power distribution data were supplied on a cycle specific basis by Carolina Power and Light Co. In applying this data in the discrete ordinates analysis, the fission spectra, neutrons released per fission, and energy release per fission accounted for the presence of both uranium and plutonium fissioning isotopes.
1.2	**End-of-Life Predictions.** Predictions of the vessel end-of-life fluence should be made with a best estimate or conservative generic power distribution. If a best estimate is used, the power distribution must be updated if changes in core loadings, surveillance measurements, or other information indicate a significant change in projected fluence values.	Projections for future operation were based on equilibrium fuel cycle data supplied by Carolina Power and Light Co. and accounted for a power uprate. Core designs will be reviewed on a cycle specific basis to assure that they are bounded by the equilibrium core used for fluence projections.

Regulatory Position	NRC Staff Position	Westinghouse Approach
1.3.1	**Spatial Representation.** Discrete ordinates neutron transport calculations should incorporate a detailed radial- and azimuthal-spatial mesh of ~2 intervals per inch radially. The discrete ordinates calculations must employ (at a minimum) an S_8 quadrature and (at least) 40 intervals per octant.	The spatial mesh used by Westinghouse in the discrete ordinates calculations exceeds the minimum requirements for radial and azimuthal mesh specified in Staff Position 1.3.1. An S_8 angular quadrature set was used in all of the cycle specific fluence calculations. An S_{16} quadrature set was also investigated as a part of the analytical uncertainty study and tested against ex-vessel measurements.
1.3.1	**Multiple Transport Calculations.** If the calculation is performed using two or more "bootstrap" calculations, the adequacy of the overlap regions must be demonstrated.	Not applicable. The "bootstrap" technique was not used in performing the discrete ordinates calculations.
1.3.2	**Point Estimates.** If the dimensions of the tally region or the definition of the average-flux region introduce a bias in the tally edit, the Monte Carlo prediction should be adjusted to eliminate the calculational bias. The average-flux region surrounding the point location should not include material boundaries or be located near reflecting, periodic, or white boundaries.	Not applicable. This staff position pertains to Monte Carlo calculations. The discrete ordinates approach was used in the Brunswick analysis.
1.3.2	**Statistical Tests.** The Monte Carlo estimated mean and relative error should be tested and satisfy all statistical criteria.	Not applicable. This staff position pertains to Monte Carlo calculations. The discrete ordinates approach was used in the Brunswick analysis.
1.3.2	**Variance Reduction.** All variance reduction methods should be qualified by comparison with calculations performed without variance reduction.	Not applicable. This staff position pertains to Monte Carlo calculations. The discrete ordinates approach was used in the Brunswick analysis.

Regulatory Position	NRC Staff Position	Westinghouse Approach
1.3.3	**Capsule Modeling**. The capsule fluence is extremely sensitive to the geometrical representation of the capsule geometry and internal water region, and the adequacy of the capsule representation and mesh must be demonstrated.	The capsule and associated structure were modeled in the discrete ordinates calculation. Adequacy of the modeling was tested by comparison with dosimetry from withdrawn surveillance capsules. Results were shown to be within the 20% uncertainty requirement specified in Regulatory Guide 1.190.
1.3.3	**Spectral Effects on RT_{NDT}**. In order to account for neutron spectrum dependence of RT_{NDT}, when it is extrapolated from the inside surface of the pressure vessel to the T/4 and 3T/4 vessel locations using the E > 1-MeV fluence, a spectral lead factor must be applied to the fluence for the calculation of ΔRT_{NDT}.	The current calculations for Brunswick Units 1 and 2 address this issue by including a calculation of iron atom displacement (dpa) distributions through the vessel wall. The dpa damage function accounts for the spectral shift toward lower energies with deeper penetration into the carbon steel vessel wall. In point of fact, these calculations are rarely used. In Regulatory Guide 1.99 Revision 2, an attenuation function intended to simulate the dpa distribution is provided. This built in function is usually used to determine values of RT_{NDT} at the T/4 and 3T/4 vessel locations.
1.3.5	**Cavity Calculations**. In discrete ordinates transport calculations, the adequacy of the S_8 angular quadrature used in cavity calculations must be demonstrated.	Assessments of the adequacy of both the S_8 angular quadrature and P_3 scattering cross-section assumptions for cavity calculations were performed as a part of the analytical sensitivity study.

Regulatory Position	NRC Staff Position	Westinghouse Approach
1.4.1, 1.4.2, 1.4.3.	**Methods Qualification**. The calculational methodology must be qualified by both (1) comparisons to measurement and calculational benchmarks and (2) an analytical uncertainty analysis. The methods used to calculate the benchmarks must be consistent (to the extent possible) with the methods used to calculate the vessel fluence. The overall calculational bias and uncertainty must be determined by an appropriate combination of the analytical uncertainty analysis and the uncertainty analysis based on the comparisons to the benchmarks.	Measurement to calculation comparisons for the PCA Pressure Vessel Simulator described in NUREG/CR-6454 and the H. B. Robinson Unit 2 Pressure Vessel Benchmark described in NUREG/CR-6453 were completed. Likewise, an analytical sensitivity study assessing the uncertainty associated with important geometric, material density, and neutron source input parameters was performed. In combination, the results of these studies establish an overall calculational uncertainty of less than 20%.
1.4.3	**Fluence Calculational Uncertainty**. The vessel fluence (1 sigma) calculational uncertainty must be demonstrated to be $\leq$ 20% for RT_{PTS} and RT_{NDT} determination. In these applications, if the benchmark comparisons indicate differences greater than 20%, the calculational model must be adjusted or a correction must be applied to reduce the difference between the fluence prediction and the upper 1-sigma limit to within 20%. For other applications, the accuracy should be determined using the approach described in Regulatory Position 1.4, and an uncertainty allowance should be included in the fluence estimate as appropriate in the specific application.	The qualification of the methodology demonstrates an uncertainty of less than 20% (1 sigma). None of the benchmarking comparisons exceeded the 20% criteria specified in Staff Positions 1 and 1.4.3. Therefore, no adjustments to the calculated results have been required.